MATHEMATICAL PERSPECTIVES

BULLETIN (New Series) OF THE AMERICAN MATHEMATICAL SOCIETY Volume 61, Number 3, July 2024, Pages 470–514 https://doi.org/10.1090/bull/1838 Article electronically published on May 15, 2024

LAGRANGIAN, GAME THEORETIC, AND PDE METHODS FOR AVERAGING G-EQUATIONS IN TURBULENT COMBUSTION: EXISTENCE AND BEYOND

JACK XIN, YIFENG YU, AND PAUL RONNEY

ABSTRACT. G-equations are popular level set Hamilton–Jacobi nonlinear partial differential equations (PDEs) of first or second order arising in turbulent combustion. Characterizing the effective burning velocity (also known as the turbulent burning velocity) is a fundamental problem there. We review relevant studies of the G-equation models with a focus on both the existence of effective burning velocity (homogenization), and its dependence on physical and geometric parameters (flow intensity and curvature effect) through representative examples. The corresponding physical background is also presented to provide motivations for mathematical problems of interest.

The lack of coercivity of Hamiltonian is a hallmark of G-equations. When either the curvature of the level set or the strain effect of fluid flows is accounted for, the Hamiltonian becomes highly nonconvex and nonlinear. In the absence of coercivity and convexity, the PDE (Eulerian) approach suffers from insufficient compactness to establish averaging (homogenization). We review and illustrate a suite of Lagrangian tools, most notably min-max (max-min) game representations of curvature and strain G-equations, working in tandem with analysis of streamline structures of fluid flows and PDEs. We discuss open problems for future development in this emerging area of dynamic game analysis for averaging noncoercive, nonconvex, and nonlinear PDEs such as geometric (curvature-dependent) PDEs with advection.

Received by the editors July 17, 2023, and, in revised form, January 31, 2024. 2020 Mathematics Subject Classification. Primary 35B27, 35B40, 35F21, 35Qxx.

Key words and phrases. Hamilton–Jacobi PDEs, noncoercivity, nonconvexity, Lagrangian and game methods, averaging, turbulent combustion.

This work was partially supported by NSF grants DMS-1952644, DMS-2000191, DMS-2309520, and AFOSR grant FA9550-16-1-0197.

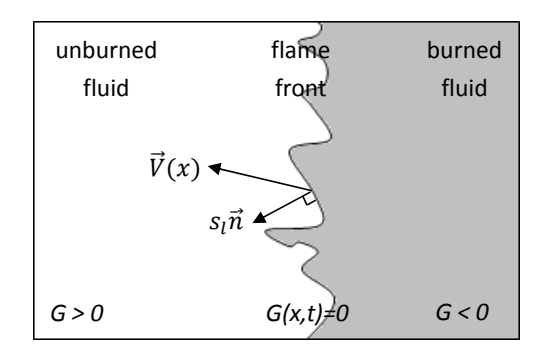


Figure 1. Level set modeling of flame propagation.

1. Introduction

Turbulent combustion is employed in practically all mobile and stationary power generation devices because turbulence increases the mass consumption rate of reactants to values much greater than laminar flames can achieve. This in turn increases the heat release rate and thus power available from a gas turbine combustor, reciprocating piston engine, or rocket motor of a given size. Few combustion engines would function without the increase in mixing and burning rates caused by turbulence. A fundamental and practically important property of a turbulent flame in a pre-mixture of reactants is how the effective propagation speed $(s_T, also called tur$ bulent flame speed) is affected by turbulence intensity among other factors including local flame front curvature, hydrodynamic strain, combustor geometry, thermal expansion, heat losses, and turbulence energy spectrum [12, 36, 89]. To date, most of our understanding of these effects in combustion science has been developed from the so-called "flamelet" models that presume the existence of a continuous flame sheet that is wrinkled by turbulence and thereby affecting the flame area, which in turn affects the mass consumption rates. The local consumption rate per unit area corresponds to the propagation rate of a planar front in the same mixture.

A well-known flamelet type model in turbulent combustion is the so called G-equation [75, 89, 111, 112], which takes the following form:

(1.1)
$$G_t + s_l |DG| + V(x) \cdot DG = 0.$$

Here $G = G(x,t) \in C(\mathbb{R}^n \times (0,\infty),\mathbb{R})$ is a reference function whose zero level set $\{x \in \mathbb{R}^n \mid G(x,t) = 0\}$ represents flame front at time t; $\{x \in \mathbb{R}^n \mid G(x,t) > 0\}$ is the unburned area and $\{x \in \mathbb{R}^n \mid G(x,t) < 0\}$ the burned area; $V \in C(\mathbb{R}^n,\mathbb{R}^n)$ is the velocity field of the ambient fluid (e.g. blowing wind in a wild fire or stirring a mixture of air and gasoline inside car engines), see Figure 1; D the spatial gradient. The motion of the flame front is driven by chemical reaction represented by the so called laminar flame speed s_l (or local burning velocity) and the ambient fluid. Hence the flame front obeys the motion law:

$$(1.2) v_{\vec{n}} = s_l + V(x) \cdot \vec{n},$$

i.e., the front speed $v_{\vec{n}}$ in the normal direction \vec{n} is the laminar flame speed (s_l) plus the projection of fluid velocity V along the normal. The s_l might not be a

constant in general, and its geometric or physical modeling leads to different types of G-equations.

The ratio of flame thickness and Kolmogorov scale (the small scale in fluid flows below which dissipation dominates) determines different combustion regions. Gequation is most suited in the so called corrugated flamelet regime where the ratio is less than one [89]. Below we derive G-equation, assuming that the G function and the flame front are smooth. Fix t > 0 and a point x on the flame front Γ_t . Let x(s) be the flame propagation route starting from x(t) = x for $s \ge t$. Then G(x(s), s) = 0 and the motion law (1.2) implies that

$$\dot{x}(s) = v_{\vec{n}(s)} \, \vec{n}(s) = (s_l + V(x(s)) \cdot \vec{n}(s)) \, \vec{n}(s),$$

where $\vec{n}(s)$ is the outward normal vector of Γ_s at x(s) that can be expressed as $\vec{n}(s) = DG(x(s),s)/|DG(x(s),s)|$. By chain rule:

$$0 = \frac{dG(x(s), s)}{ds} = G_t + DG \cdot \dot{x}(s) = 0.$$

Plugging in (1.3) immediately gives G-equation (1.1), which was formally introduced by Williams [111,112] in 1985, although the above derivation and an earlier form of G-equation first appeared in Markstein's work [75] in 1964. We also note that the G-equation model and crystal growth front propagation model served as two major sources in the systematic mathematical development of the level-set method by Osher and Sethian [88].

Two observations are in order.

(1) The reference function G(x,t) has no physical meaning except its zero level set (called nonreactive in combustion literature). Solutions to G-equations are in general not C^1 although the equation is derived under smoothness assumptions. Mathematically, the solutions need to be defined in the sense of viscosity solutions whose basic definition and backgrounds are in Section 2, providing mathematical foundation of level set equations. In particular, the choice of different reference functions does not impact the zero level set. Precisely speaking, if both \tilde{G} and G are solutions to equation (1.1) subject to

$$\{x \in \mathbb{R}^n \mid \tilde{G}(x,0)\} = \{x \in \mathbb{R}^n \mid G(x,0)\}$$

then

$$\{x \in \mathbb{R}^n \mid \tilde{G}(x,t) = 0\} = \{x \in \mathbb{R}^n \mid G(x,t) = 0\}$$

for all t > 0. An intuitive way to understand this is that G is a solution if and only if $\tilde{G} = f(G)$ is also a solution for any differentiable function $f : \mathbb{R} \to \mathbb{R}$ satisfying f' > 0. See [27,44] for rigorous proofs.

(2) In more comprehensive combustion models, fluid velocity and chemical transport are determined by a coupled system of Navier–Stokes and reaction-diffusion-advection equations, which is called the direct method. A flamelet approach based on G-equations neglects the effects of thermal expansion (and so the above two-way coupling between the flame and turbulent flow field) as well as heat losses but may retain curvature and strain dependence on s_l in the G-equation formulation. In the simplified setting of G-equation, the fluid velocity (turbulent flow field) is prescribed with the focus to understand how the flame propagates in an ambient fluid. Such an approach is known as passive modeling, making it more feasible to theoretically study (so called "pencil and paper") or compute the impacts of

significant factors in combustion, e.g., flow perturbation, flame intensity, and flame stretch. That the passive modeling may yield physically meaningful results has been demonstrated by experiments [1,94,99] that employ aqueous autocatalytic chemical reactions rather than gaseous flames because the thermal expansion and heat loss effects are absent in the aqueous mixtures.

To initiate a practical simulation of G-equation for turbulent flows, solutions of Navier–Stokes equations are often computed first to set up the velocity field V. For numerical approximations of G-equations and applications in combustion, we refer to [58, 62, 66, 70, 87, 88, 124] among others.

1.1. **Different types of G-equations.** In general, the local burning velocity s_l depends on flame stretch [89]:

$$(1.4) s_L = (s_L^0 - d s_L^0 \kappa + d \vec{n} \cdot S \cdot \vec{n})_+.$$

See [89, Section 2.6] for a formal derivation of relevant expressions from the reaction-diffusion-advection equations. Here

- s_L^0 is a positive constant representing the laminar flame speed of the unstretched flame. The positive part $(a)_+ = \max\{a,0\}$ is imposed to avoid negative laminar flame speed since materials cannot be "unburned". This correction usually is not explicitly mentioned in combustion literature since, by default, the laminar flame speed is always assumed to be nonnegative there. However, mathematically, large positive curvature κ or negative strain rate $\vec{n} \cdot S \cdot \vec{n}$ could occur as time evolves. Hence it is necessary to explicitly add $(\cdot)_+$ if physical validity is taken into consideration in the modeling of flame propagation [9, 124];
- the expression $-ds_L^0 \kappa + d\vec{n} \cdot \vec{S} \cdot \vec{n}$ represents the correction due to flame stretching. The constant d is the Markstein length which is proportional to laminar flame thickness. Intuitively speaking, the local burning velocity is affected by chemical reactions (or burning temperature) and heat release that are related to the surface area of the flame front. Suppose that a smooth hypersurface in \mathbb{R}^n is moving in the velocity field V. Then the front surface stretch rate is

$$\frac{1}{\sigma} \frac{d\sigma}{dt} = \operatorname{div}(V) - \vec{n} \cdot S \cdot \vec{n}.$$

Here σ is the surface element area. The derivation of the above formula could be found in [70,76].

The first correction term $-d s_L^0 \kappa$ in (1.4) describes the curvature effect [74,75,89], where

$$\kappa = \operatorname{div}\left(\frac{DG}{|DG|}\right)$$

is the mean curvature of the flame surface.

The second correction term $d\vec{n} \cdot S \cdot \vec{n}$ in (1.4) quantifies the straining effect on the flame from the flow [70,76]. The normal vector \vec{n} at the flame surface points in the direction of the unburned region, and

$$S = \frac{DV + (DV)^{\top}}{2}$$

is called the strain rate tensor.

For convenience, we set the constant

$$s_L^0 = 1$$

throughout this paper.

If (1.4) is plugged into equation (1.1), the general G-equation is a second order quasilinear parabolic equation:

(1.5)
$$G_t + H(D^2G, DG, x) = 0,$$

where the associated Hamiltonian is

$$H(M, p, x) = \left(|p| - d\left(\operatorname{tr}M - \frac{p \cdot M \cdot p}{|p|^2} - \frac{p \cdot S \cdot p}{|p|}\right)\right)_{+} + V(x) \cdot p$$

for $(M,p) \in S^{n \times n} \times (\mathbb{R}^n \setminus \{0\})$. At p=0, following [33], H(M,0,x) is set to 0 for subsolutions and $2dn\|A\|$ for supersolutions. Here $S^{n \times n}$ is the space of $n \times n$ real symmetric matrices. Note that H is monotonically nonincreasing with respect to M, noncoercive $(H \not\to +\infty \text{ as } |p| \to +\infty \text{ if } |V| > 1)$ and nonconvex with respect to the p variable if d > 0.

For simplicity, we will treat curvature and strain terms separately.

1.1.1. Inviscid G-equation (d = 0). In the basic setting, the local burning velocity s_l is taken to be a constant $(s_l = s_L^0 = 1)$, i.e., ignore the curvature effect and strain rate by letting d = 0. The corresponding G-equation is then a first-order convex but in general noncoercive (if |V| > 1) Hamilton–Jacobi equation (HJE):

$$G_t + |DG| + V(x) \cdot DG = 0.$$

In this situation, the laminar flame speed could depend on locations, i.e., $s_l = a(x)$ for some positive function a(x). A notable example is the celebrated Rothermel surface fire spread model for forest fires [3], where a(x) depends on the landscape (uphill or downhill) and the types of plants there. Due to diffusion in a numerical scheme or artificial viscosity to stabilize computation [54,60,87], it is of interest to assess such effects by considering the viscous version of G-equation

$$(1.6) -d\Delta G + G_t + |DG| + V(x) \cdot DG = 0,$$

where the Laplacian term mimics numerical diffusion. The Laplacian term is also found to be relevant for representing the effect of thermal relaxation under transverse heat diffusion in the preheat zone of a wrinkled front [30, 54]. Moreover, the viscous G-equation (1.6) is adopted for dynamic modeling of large eddy simulation of turbulent premixed combustion in homogeneous isotropic turbulence in [54]. Surprisingly, such a second order regularization at any small d > 0 acts as a singular perturbation drastically altering the effective burning velocity; see [69] for a mathematical proof and [54, Figure 1] for numerical observations.

1.1.2. Curvature G-equation. Geometry on the flame front provides a phenomenological way to describe the change of temperature along the flame front, which impacts the rate of chemical reactions and hence the local burning speed. Intuitively, it says that if the flame front bends toward the cold region (un-burned area, point C in Figure 2), the flame propagation slows down. If the flame front bends toward the hot spot (burned area, point B in Figure 2), it burns faster.

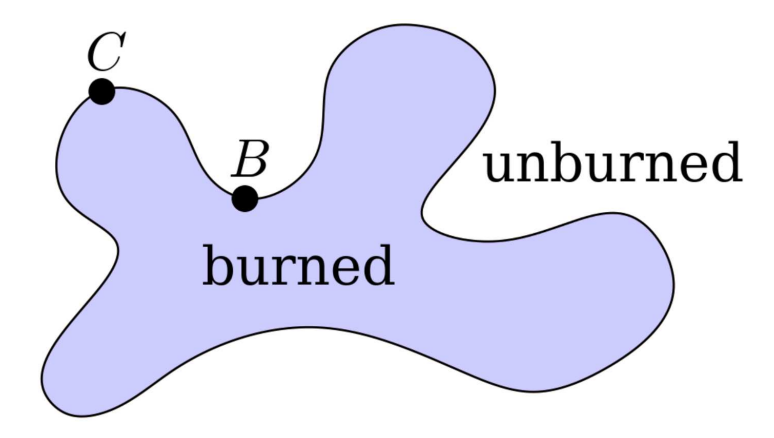


FIGURE 2. Curvature effect: faster burn at B (bending towards hot region) than C.

There is a vast literature in turbulent combustion discussing the impact of curvature effect. Below is the most recognized empirical linear relation first proposed by Markstein [74,75] (see also [89]):

$$(1.7) s_l = s_L^0 (1 - d \kappa)_+.$$

Here the strain rate term in (1.4) is ignored. This correction leads to a mean curvature type equation with advection:

(1.8)
$$G_t + \left(1 - d\operatorname{div}\left(\frac{DG}{|DG|}\right)\right)_+ |DG| + V(x) \cdot DG = 0.$$

This equation has both nonconvex and noncoercive nature. Moreover, due to the presence of the physical cut-off ()₊, this quasilinear parabolic equation is highly degenerate, causing nonexistence of effective burning velocity in 3D flows (see Section 4.4).

1.1.3. Strain G-equation. By setting $s_L^0=1$, the expression for laminar speed is

$$(1.9) s_L = (1 + d \, \vec{n} \cdot S \cdot \vec{n})_+.$$

This leads to a nonconvex-noncoercive first order HJE:

(1.10)
$$G_t + \left(1 + d \frac{DG \cdot S(x) \cdot DG}{|DG|}\right)_+ |DG| + V(x) \cdot DG = 0.$$

Nonconvex first order Hamilton–Jacobi equations first appeared in zero sum twoperson differential games [40,55]. The strain G-equation provides a natural physical example. Although there is a large volume of combustion literature investigating the strain rate effect, there is not much mathematical work studying the above PDE, a nonconvex HJE with physical meaning.

1.2. Turbulent burning velocity and homogenization of G-equation. Effective burning velocity (a.k.a. turbulent flame speed) is one of the most fundamental quantities in turbulent combustion. Roughly speaking, it is the flame propagation speed after averaging the fluctuations around the mean flame front. Establishing its existence rigorously has, in general, remained an open problem. Below are two equivalent perspectives to describe it from the G-equation. Fix a unit direction

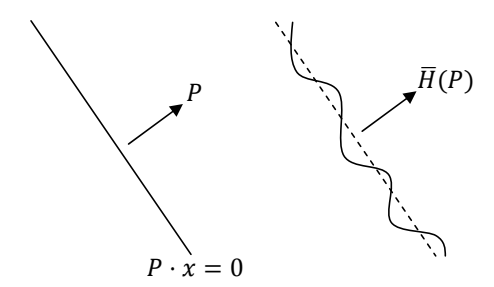


FIGURE 3. A classical (left) vs. an effective (right, dashed) planar front by averaging an oscillatory flame front (right, solid).

 $p \in \mathbb{R}^n$. Assume that the initial flame front is planar $\{x \in \mathbb{R}^n \mid G(x,0) = x\} = \{x \in \mathbb{R}^n \mid p \cdot x = 0\}$. Due to the motion of the ambient fluid, the flame front wrinkles as time evolves, see Figure 3.

Perspective 1. The mean flame front is still planar and might eventually propagate with a steady speed $s_T(p)$.

Mathematically, this implies that

$$(1.11) G(x,t) \approx p \cdot x + v(x) - t s_T(p),$$

where the right-hand side is an approximate traveling wave solution of the G-equation. The $s_T(p)$, if it exists, is the effective Hamiltonian $s_T(p) = \overline{H}(p)$ (see Figure 3) associated with the G-equation (a first or second order HJE), defined in a nonlinear eigenvalue problem (a.k.a. cell or corrector problem [41,67]):

(1.12)
$$H(D^2v, p + Dv, x) = (\text{or } \approx)\overline{H}(p) \text{ in } \mathbb{R}^n$$

where v is called a corrector (eigenfunction), and \bar{H} the eigenvalue. Here \approx refers to approximate solutions when exact solutions do not exist. See Section 2 for more details.

In general, the speed $\overline{H}(p)$ is direction p dependent or anisotropic. Moreover, except in some simple cases (e.g., 2D shear flows), there is no closed form formula of \overline{H} . If $\overline{H}(p)$ exists, we have:

(1.13)
$$\overline{H}(p) = -\lim_{t \to \infty} \frac{G(x,t)}{t},$$

where G is the solution to the corresponding equation (1.1) subject to $G(x,0) = p \cdot x$. Formula (1.13) can be used to numerically compute $\overline{H}(p)$, see [58, 70, 90].

Perspective 2. In combustion literature and experiments, the ratio s_T/s_l is measured by the ratio between the surface area of the wrinkled flame front and the flat one (unwrinkled). According to [60, equations (11) and (12)], the turbulent flame speed at time t is approximately the volume average

$$u_T(t) = \int_{[0,1]^n} s_l |DG(x,t)| dx$$

when the flow field V is 1-periodic, incompressible with mean zero (see [24] for relevant discussions). Integrating (1.1) over x gives

$$\int_{[0,1]^n} s_l |DG(x,t)| \, dx = -\int_{[0,1]^n} G_t(x,t) \, dx.$$

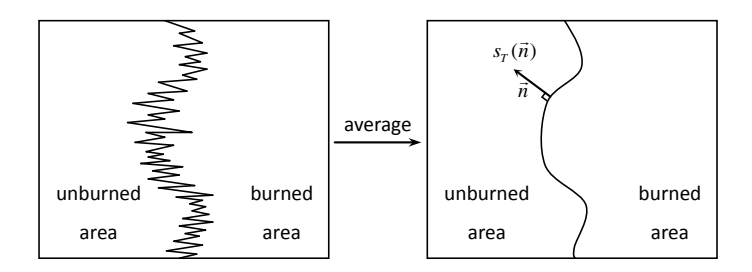


FIGURE 4. Averaging fluctuations around a general flame front.

Then the time average of u_T is

$$\frac{1}{t} \int_0^t u_T(s) \, ds = -\frac{\int_{[0,1]^n} \left(G(x,t) - p \cdot x \right) dx}{t} \underset{t \gg 1}{\sim} -\frac{\int_{[0,1]^n} G(x,t) \, dx}{t}.$$

As noted in [60], an open problem is whether the time average of u_T converges to a constant as $t \uparrow \infty$, or the validity of the spatially averaged version of (1.13). A computational example in [60] based on solutions of Navier–Stokes equations for the flow velocity V showed the convergence of the time-averaged u_T .

The existence of $\overline{H}(p)$ usually leads to the following full homogenization result in the single small scale situation [42]. Denote by ϵ the Kolmogorov scale. Change variables

$$x \to \frac{x}{\epsilon}$$
, $V(x) \to V\left(\frac{x}{\epsilon}\right)$ and $d \to d\epsilon$

and denote by $G^{\epsilon}(x,t)$ the corresponding solution to (1.1) with the prescribed initial flame front G(x,0)=g(x). Then

$$\lim_{\epsilon \to 0} G^{\epsilon}(x,t) = \bar{G}(x,t),$$

where $\bar{G}(x,t)$ solves an effective equation

$$\begin{cases} \bar{G}_t + \overline{H}(D\bar{G}) = 0\\ \bar{G}(x,0) = g(x). \end{cases}$$

Following standard notations, we write $s_T(p) = \overline{H}(p)$. The effective equation says that the averaged flame front will propagate with speed

$$v_{\vec{n}} = \overline{H}(\vec{n})$$

along its normal direction \vec{n} . See Figure 4 for an illustration.

We shall focus on the following two topics closely related to a central theme in combustion (how fast can it burn?).

(1) Proving the existence of $\overline{H}(p)$ under physically meaningful assumptions. This is equivalent to finding solutions or approximate solutions of the form (1.11), which reduces to studying cell problems in homogenization theory of HJE [41,67]. Due to the lack of coercivity from a large flow, standard PDE methods are insufficient. The Lagrangian approaches are introduced, especially game theoretic methods in the presence of nonconvexity from curvature and flame stretching effects.

- (2) Studying qualitative and quantitative properties of $\overline{H}(p)$ beyond existence, a mathematical topic of physical impact. Below are two issues addressed in a large body of combustion literature through theoretical or empirical approaches.
 - (a) Dependence of the turbulent burning velocity on flow intensity. Precisely speaking, scale the flow field V to AV by a positive constant A and inquire about the growth behavior of $\overline{H}(p)$ as $A \to +\infty$. This is one of the major approaches to speed up flame propagation within a combustion vessel.
 - (b) Understanding how the turbulent burning velocity relies on the curvature and strain effect. In particular, an important problem in turbulent combustion is whether adding the curvature correction will decrease the prediction of the turbulent burning velocity. This is equivalent to asking whether \overline{H} is a monotonically decreasing function of the Markstein length (or Markstein number) d in (1.4) that mainly depends on the type of burning fuel.

Tackling (a) and (b) often calls for challenging analysis of the underlying dynamical systems (e.g., on flow geometry and asymptotics), which can be made precise without making general assumptions by studying specific flows with physical origin. The two common candidates to start with are shear flows and two dimensional (2D) cellular flows. Even for 2D shear flow where the PDE under study basically reduces to ordinary differential equation (ODE), the associated mathematical questions could be highly nontrivial when curvature terms are involved. In the next step to analyze 3D flows, we choose a well-known example, the Arnold–Beltrami–Childress (ABC) flow [7,29,35,47], a steady solution to the 3D Euler equation with chaotic yet nonergodic streamlines. The integrable case of the ABC flow is the 2D cellular flow (a.k.a. BC flow). Recent progress in constructing ballistic orbits [58,77,120] is necessary to address issue I for the inviscid G-equation in the ABC flow.

For curvature and strain G-equations, our integrated Lagrangian and Eulerian methodology established first for the inviscid G-equation continues to shine in a two-player game framework in the non-convex setting. Even though the classical Euler-Lagrange duality via Legendre transform is missing, the success of our blended Lagrangian-Eulerian analysis points to a *subtle and hidden duality* for future research to explore in geometric PDEs and flows. On the other hand, for the curvature G-equations in three and higher dimensions, the averaging (homogenization) breaks down in large enough intensity shear flows [79], indicating a non-convex phenomenon that an existence proof for the effective burning speed through volume preserving (incompressible) flows is dimension and flow dependent.

Outline of the paper. In Section 2, we review the basics of viscosity solutions and homogenization theory. In Sections 3–4, we discuss different types of G-equations, present theoretical and numerical results for the basic and curvature G-equations based on control and two-player game representations as well as PDE methods. Section 5 gives a two-player differential game and PDE analysis for the strain G-equation. Section 6 revisits other passive scalar flame propagation models related to G-equation. Section 7 is a brief overview of stochastic homogenization and multiscale modeling of the basic G-equation in turbulent combustion. Conclusions are in Section 8. The open problems appear along the way.

2. Preliminary: Viscosity solutions and homogenization

For the reader's convenience, we will review some basic concepts and techniques about viscosity solutions and homogenization theory most relevant to problems discussed in this paper. See [33, 38, 39, 104] for more details.

Consider a general second order Hamilton–Jacobi equation (HJE)

$$(2.1) u_t + H(D^2u, Du, u, x) = 0 \text{on } \mathbb{R}^n \times (0, \infty).$$

Here the Hamiltonian H = H(M, p, z, x) is a function defined on $(M, p, z, x) \in S^{n \times n} \times \mathbb{R}^n \times \mathbb{R} \times \mathbb{R}^n$, where $S^{n \times n}$ is the set of $n \times n$ symmetric matrices. We say that the Hamiltonian H is coercive in the gradient variable p if for any fixed $K \geq 0$,

$$\lim_{|p|\to +\infty} \min_{|M|+|z|+|x|\le K} H(M,p,z,x) = +\infty.$$

Definition 2.1. An upper semicontinuous function u(x,t) defined on $\mathbb{R}^n \times (0,\infty)$ is called a viscosity subsolution of (2.1) if for any $\phi \in C^2(\mathbb{R}^n \times (0,\infty))$ and any point $(x_0,t_0) \in \mathbb{R}^n \times (0,\infty)$, when

$$0 = \phi(x_0, t_0) - u(x_0, t_0) \le \phi(x, t) - u(x, t)$$

holds for (x,t) in a neighborhood of (x_0,t_0) , we have

$$\phi_t(x_0, t_0) + H(D^2\phi(x_0, t_0), D\phi(x_0, t_0), \phi(x_0, t_0), x_0) \le 0.$$

Definition 2.2. A lower semicontinuous function u(x,t) defined on $\mathbb{R}^n \times (0,\infty)$ is called a viscosity supersolution of (2.1) if for any $\phi \in C^2(\mathbb{R}^n \times (0,\infty))$ and any point $(x_0,t_0) \in \mathbb{R}^n \times (0,\infty)$, when

$$0 = \phi(x_0, t_0) - u(x_0, t_0) \ge \phi(x, t) - u(x, t)$$

holds for (x,t) in a neighborhood of (x_0,t_0) , we have

$$\phi_t(x_0, t_0) + H(D^2\phi(x_0, t_0), D\phi(x_0, t_0), \phi(x_0, t_0), x_0) \ge 0.$$

Definition 2.3. A continuous function u(x,t) defined on $\mathbb{R}^n \times (0,\infty)$ is called a viscosity solution of (2.1) if it is both a viscosity subsolution and a viscosity supersolution.

Similarly, we can define viscosity subsolutions, supersoltutions, and solutions for steady state equations

(2.2)
$$H(D^2u, Du, u, x) = 0$$
 on U ,

where U is an open subset of \mathbb{R}^n .

Moreover, we say that (2.2) has approximation solutions if for any $\delta > 0$, there is a continuous function $u_{\delta}(x,t)$ that satisfies the following inequality in the viscosity sense

(2.3)
$$-\delta \le H(D^2 u^{\delta}, D u^{\delta}, u^{\delta}, x) \le \delta \quad \text{on } \mathbb{R}^n \times (0, \infty).$$

The notion of viscosity solutions provides a rigorous mathematical framework to describe the correct "physical" solution of the corresponding equations (2.1) or (2.2) when classical solutions might not exist. Important examples include first order HJ equations or second order degenerate elliptic equations arising from control theory or front propagation problems in applications. Heuristically, the name comes from the vanishing viscosity method. To stabilize the equation numerically, an artificial viscosity term is added to the equation, although often without clear

physical meanings. Precisely speaking, given h > 0, let u^h be a smooth solution (if it exists) to

$$-h \Delta u^h + u_t^h + H(D^2 u^h, D u^h, u^h, x) = 0 \quad \text{on } \mathbb{R}^n \times (0, \infty)$$

with given initial data $u^h(x,0) = g(x)$. Then it is natural to expect that u^h converges to the correct physical solution of (2.1) as $h \to 0$ (vanishing viscosity). In fact, using maximum principle, it is not hard to prove that if

$$\lim_{h\to 0} u^h(x,t) = u(x,t) \quad \text{locally uniformly in } \mathbb{R}^n \times (0,\infty),$$

then u is the viscosity solution to (2.1) subject to u(x,0) = g(x). A similar limiting process can also be carried out for the steady case (2.2) with given boundary data u on ∂U . Although this vanishing viscosity limit is intuitively clear, the existence of viscosity solutions is usually established by Perron's method, which is more convenient. Under suitable assumptions, uniqueness of viscosity solutions holds with prescribed initial data or boundary data. We refer to [33] for more details.

Next, we review the basics of homogenization of nonlinear equations that started from [67]. In our context, assume that H = H(M, p, x) is periodic in x and consider the solution u^{ϵ} to the oscillatory equation

(2.4)
$$\begin{cases} u_t^{\epsilon} + H\left(\epsilon D^2 u^{\epsilon}, D u^{\epsilon}, \frac{x}{\epsilon}\right) = 0 & \text{in } \mathbb{R}^n \times (0, \infty) \\ u^{\epsilon}(x, 0) = g(x). \end{cases}$$

when the underlying environment has small scale $\epsilon > 0$. Here we omit the dependence on the u variable for convenience. Under proper assumptions, it can be shown [42,67] that

(2.5)
$$\lim_{\epsilon \to 0} u^{\epsilon}(x,t) = u(x,t) \quad \text{locally uniformly in } \mathbb{R}^{n} \times (0,\infty).$$

Here u(x,t) is the unique continuous viscosity solution to the effective equation

(2.6)
$$\begin{cases} \bar{u}_t + \overline{H}(D\bar{u}) = 0\\ \bar{u}(x,0) = g(x). \end{cases}$$

The above limiting process is called homogenization. Given $p \in \mathbb{R}^n$, the effective Hamiltonian $\overline{H}(p) : \mathbb{R}^n \to \mathbb{R}$ is the unique number such that the following cell (corrector) problem

(2.7)
$$H(D^{2}v, p + Dv, x) = \overline{H}(p) \text{ in } \mathbb{R}^{n}$$

has a continuous \mathbb{Z}^n -periodic viscosity solution (or approximate solutions in the sense of (2.3)) v(x), which is called a corrector. Here we would like to stress that the solution v in general might not be unique even up to an additive constant. When the original Hamiltonian H is from front propagation problems, the effective Hamiltonian \overline{H} has a clear physical meaning of effective propagation speeds in the corresponding setting. For the mechanical Hamiltonian $H(p,x) = \frac{1}{2}|p| + V(x)$, the effective Hamiltonian and the associated cell problem have helped construct quasi-modes of Schrödinger operators via various quantization procedures [43].

If the existence of the cell problem can be established (i.e., existence of effective Hamiltonian), then the convergence (2.5) usually follows from the perturbed test function method [41,42]. Moreover, comparison principle implies that if the initial

value $u(x,0) = p \cdot x$, then

(2.8)
$$-\lim_{t \to +\infty} \frac{u(x,t)}{t} = \overline{H}(p) \quad \text{for all } x \in \mathbb{R}^n.$$

Technically speaking, the key part is to establish the existence of the cell problem (2.7). Below is the mechanism first introduced in [42,67]: for $\lambda > 0$, let v_{λ} be the unique periodic viscosity solution of

$$\lambda v_{\lambda} + H(D^2 v_{\lambda}, p + D v_{\lambda}, x) = 0$$
 in \mathbb{R}^n .

Then show that

$$-\lim_{\lambda \to 0} \lambda \, v_{\lambda}(x) = \text{ a constant } \text{ for } x \in \mathbb{R}^n.$$

This constant, if it exists, is the effective Hamiltonian $\overline{H}(p)$. To prove the above, it suffices to show that the oscillation of v_{λ} is uniformly bounded:

(2.9)
$$\max_{x,y \in \mathbb{R}^n} |v_{\lambda}(x) - v_{\lambda}(y)| \le C$$

for a constant C independent of λ . The standard approach to prove the uniform bound is to derive equicontinuity of $v_{\lambda}(x)$ for $\lambda \in [0,1]$ (e.g., uniform Hölder continuity [67]). Then $v = \lim_{\lambda \to 0} (v_{\lambda}(x) - v_{\lambda}(0))$ (up to a subsequence if necessary) is a solution to the cell problem.

However, when H is not coercive in the gradient variable p or is only degenerate elliptic in the Hessian variable M, like the curvature G-equation, the equicontinuity is usually not valid. There appears no systematic way to obtain (2.9). Customized methods based on the structure of equations are often needed, often relying on approximate solutions of the cell problem (2.7) in the sense of (2.3).

From a numerical point of view [38], the effective equation can be used to approximate the original oscillatory equation (2.4) where the computation is very expensive in order to resolve the small scale ϵ . Of course, one has to first compute the effective Hamiltonian $\overline{H}(p)$, which can be viewed as some sort of nonlinear averaging of the original Hamiltonian. However, even for simple cases like $H(p,x) = \frac{1}{2}|p|^2 + V(x)$ or H(p,x) = a(x)|p|, the effective Hamiltonian does not have close-form formulas except in 1D. Various numerical schemes [58, 70, 90] have been developed to compute $\overline{H}(p)$ based on the large time limit (2.8).

Understanding nontrivial analytic properties of the effective Hamiltonian is extremely challenging and often requires deep tools beyond standard PDE techniques. Such kinds of problems have been studied for decades in the areas of first passage percolation in probability theory, stable norm/ β -functions in geometry, and dynamical systems, which are essentially effective Hamiltonian in the corresponding context. We refer to [105] and references therein for more discussion about such connections. Nevertheless, there are not many relevant works in the PDE literature. See [57,106] for recent progress in this direction. In particular, it is surprising to see that local properties of \overline{H} could be dramatically different from the original Hamiltonian. For example, when n=2, for generic potential function V, the effective Hamiltonian $\overline{H}(p)$ associated with $H(p,x)=\frac{1}{2}|p|^2+V(x)$ is piecewise 1D for p in a dense open set $U\subset\mathbb{R}^2$ ([122]).

Finally, we would like to mention that there is a large body of literature and active research on homogenization of scalar conservation laws and Hamilton–Jacobi PDEs in random environments (see [92,102,110] for early works). It is an interesting question to explore how stochastic modeling of turbulent flows V in practical

situations is related to typical mathematical assumptions in stochastic homogenization. In this survey paper, we will mainly focus on the periodic setting, with the stochastic aspects of G-equation briefly reviewed in Section 7.

3. Inviscid G-equation: The basic case

Let G(x,t) be the unique viscosity solution to the inviscid G-equation

(3.1)
$$\begin{cases} G_t + |DG| + V(x) \cdot DG = 0 & \text{on } \mathbb{R}^n \times (0, \infty), \\ G(x, 0) = g(x). \end{cases}$$

As a solution to a convex HJE, G(x,t) has a control formula [39]:

(3.2)
$$G(x,t) = \inf_{\alpha \in \mathcal{A}_t} g(\xi_{\alpha}(t)).$$

Here A_t is the set of measurable functions $\alpha = \alpha(s) : [0, t] \to \overline{B_1(0)}$ and ξ_{α} is the Lipschitz continuous curve satisfying

$$\begin{cases} \dot{\xi}_{\alpha}(s) = -V(\xi_{\alpha}(s)) + \alpha(s) & \text{for a.e. } s \in [0, t] \\ \xi_{\alpha}(0) = x. \end{cases}$$

See [39] for connections between general convex Hamilton–Jacobi equations and control theory. We define the following reachability notion.

Definition 3.1. Given $x, y \in \mathbb{R}^n$, we say that y is reachable from x within time T if there exists a Lipchitz continuous curve $\xi : [0,T] \to \mathbb{R}^n$ such that $\xi(0) = x$, $\xi(T) = y$ and $|\dot{\xi}(s) + V(\xi(s))| \le 1$ for a.e. $s \in [0,T]$.

Then we have the following one-sided bound.

Lemma 3.2. Suppose that u is a viscosity subsolution to

$$|Du| + V(x) \cdot Du \le C$$
 in \mathbb{R}^n

for some fixed constant C. If y is reachable from x within time T, then

$$u(x) \le u(y) + CT$$
.

Proof. For convenience, we may assume that u and the curve ξ connecting x and y are both C^1 . Then

$$\frac{du(\xi(t))}{dt} = Du \cdot \dot{\xi} \ge -V(\xi) \cdot Du - |Du| \ge -C.$$

Hence

$$u(y) - u(x) = \int_0^T \frac{du(\xi(t))}{dt} \ge -CT.$$

3.1. Homogenization of inviscid G-equation. For convenience, we assume that the flow field V is \mathbb{Z}^n -periodic, C^1 and incompressible (i.e., $\operatorname{div}(V)=0$). The incompressiblity assumption can be relaxed. Meanwhile, it is easy to give examples of smooth V where homogenization fails. The following homogenization result of inviscid G-equation was proved independently in [116] and [22] through distinct methods. For $\epsilon>0$, let $G^\epsilon(x,t)$ be the solution to

(3.3)
$$\begin{cases} G_t^{\epsilon} + |DG^{\epsilon}| + V\left(\frac{x}{\epsilon}\right) \cdot DG^{\epsilon} = 0 & \text{on } \mathbb{R}^n \times (0, \infty) \\ G^{\epsilon}(x, 0) = g(x). \end{cases}$$

Theorem 3.3.

$$\lim_{\epsilon \to 0} G^{\epsilon}(x,t) = \bar{G}(x,t) \quad locally \ uniformly \ on \ \mathbb{R}^n \times (0,\infty).$$

Here \bar{G} is the unique viscosity solution to the effective equation

(3.4)
$$\begin{cases} \bar{G}_t + \overline{H}(D\bar{G}) = 0 & on \ \mathbb{R}^n \times (0, \infty), \\ \bar{G}(x, 0) = g(x). \end{cases}$$

 $\overline{H}(p) \in C(\mathbb{R}^n, [0, \infty))$ is a convex positive homogeneous function of degree one and satisfies the enhancement property, i.e., $\overline{H}(p) \geq |p|$.

3.1.1. Sketch of proof. As mentioned in Section 2, the key is to prove the existence of periodic solution or approximate solution to the cell problem for any given vector $p \in \mathbb{R}^n$:

$$|p + Dv| + V(x) \cdot (p + Dv) = \overline{H}(p)$$
 in \mathbb{R}^n .

Below we present the method in [116] with a slightly refined version in [119].

Step 1. Consider the λ -auxiliary equation for $\lambda > 0$:

$$\lambda v_{\lambda} + |p + Dv_{\lambda}| + V(x) \cdot (p + Dv_{\lambda}) = 0.$$

The goal is to show that

$$\lim_{\lambda \to 0} \lambda \, v_{\lambda}(x) = \text{constant} \quad \text{uniformly on } \mathbb{R}^n.$$

This will follow immediately if we can establish the uniform boundedness of the oscillation:

$$\max_{x,y \in \mathbb{R}^n} |v_{\lambda}(x) - v_{\lambda}(y)| \le C$$

for a constant C independent of λ . Due to the lack of coercivity, the standard uniform Lipschitz continuity estimate of v_{λ} is not available. To overcome that, we consider

$$\bar{v}(x) = \limsup_{y \to x, \ \lambda \to 0} \lambda \ v_{\lambda}(y).$$

Then routine argument shows that \bar{v} is an upper semicontinuous solution to

$$|D\bar{v}| + V(x) \cdot D\bar{v} \le 0.$$

Integrating over the unit cube $Q_1 = [0,1]^n$ on both sides leads to

$$\int_{Q_1} |D\bar{v}| \, dx = 0.$$

Accordingly, $|D\bar{v}| \equiv 0$ and $\bar{v}(x) = \text{constant that is denoted by } v^*$.

Step 2. For $x \in \mathbb{R}^n$, set

$$\underline{v}(x) = \lim_{y \to x} \inf_{\lambda \to 0} \lambda \ v_{\lambda}(y).$$

Due to the convexity of the Hamiltonian $H(p, x) = |p| + V(x) \cdot p$ with respect to p, $h_{\lambda}(x) = -v_{\lambda}$ is a viscosity subsolution to

$$-\lambda h_{\lambda} + |p - Dh_{\lambda}| + V(x) \cdot (p - Dh_{\lambda}) \le 0.$$

Note that this is in general not true for viscosity solutions of nonconvex HJ equations. Similar to Step 1, $\limsup_{\lambda\to 0} \lambda \, h_\lambda(x) = -\underline{v}(x)$ is a constant. Hence $\underline{v}(x) = \text{constant}$ that is denoted by v_* .

Obviously, $v_* \leq v^*$. It suffices to prove that

$$v_* > v^*$$

By choosing a suitable subsequence of λ , this follows from Step 3 and Lemma 3.2.

Step 3. It is easy to see that for any $x \in \mathbb{R}^n$, there exist $y \in \mathbb{R}^n$, r > 0 and T > 0 such that for every pair $(x', y') \in B_r(x) \times B_r(y)$, y' is reachable from x' within time T.

Remark 3.4. The above method and conclusion can be easily extended to the time dependent case where V=V(x,t) and is periodic in (x,t). The key is to recover Step 1, i.e., showing that the limsup is a constant. The other parts are similar. In fact, assume that $\bar{v}(x,t)$ is periodic in both time and space and a viscosity subsolution to

$$\bar{v}_t + |D\bar{v}| + V(x,t) \cdot D\bar{v} < 0$$
 on $\mathbb{R}^n \times \mathbb{R}$.

As in Step 1, integrating with respect to both x and t on $Q_1 \times [0, 1]$ leads to $D\bar{v} = 0$, i.e., \bar{v} is constant in x. Then $v_t \leq 0$, which implies that \bar{v} is also constant in t due to the periodicity in t.

3.1.2. Optimal convergence rate $O(\epsilon)$. We expect to obtain the optimal convergence rate $O(\epsilon)$ if the initial data g is Lipschitz continuous:

$$(3.5) |G^{\epsilon}(x,t) - \bar{G}(x,t)| \le O(\epsilon).$$

This $O(\epsilon)$ optimal convergence rate has been established in [105] for general coercive convex Hamilton–Jacobi equations. See [105] and references therein for other important works in this topic.

Below we list the main steps with details left to the interested readers to explore. It is enough to prove this for (x, t) = (0, 1).

Step 1. For $x, y \in \mathbb{R}^n$, define a distance function

$$d(x,y) =$$
the minimum time to reach y from x .

See [23, 81] for some interesting estimates about d(x, y) although we only need $d(x, y) < \infty$ for our purpose. Note that d might not be continuous due to the lack of coercivity.

Step 2. This is the key step. Due to [13] and the corresponding connections elaborated in [105], there exists a continuous function $\bar{d}(x,y)$ such that

$$\left|\epsilon d\left(0,\frac{x}{\epsilon}\right) - \bar{d}(0,x)\right| \leq C\epsilon |x|$$

for a constant C independent of ϵ . We want to point out that to establish the upper bound $\epsilon d\left(0, \frac{x}{\epsilon}\right) \leq \bar{d}(0, x) + C\epsilon |x|$ is not very hard. The main difficulty is to verify the other direction that relies on a surprising and beautiful cutting lemma [13, Lemma 2]. Then (3.5) should follow by establishing connection between (3.2) and the control formulation of the solution to the effective equation (3.4) by the approach in [81].

3.2. Explicit formula of $\overline{H}(p)$ in 2D shear flows. For 2D shear flow V (e.g., the flow within a slot burner), we obtain the explicit formula of $\overline{H}(p)$. Let $V(x_1, x_2) = (0, f(x_1))$ for a continuous periodic function $f : \mathbb{R} \to \mathbb{R}$. Given p = (a, b), the corresponding cell problem reduces to the ODE:

$$\sqrt{(a+v'(y))^2+b^2}+b\,f(y)=\overline{H}(p),$$

where $v: \mathbb{R} \to \mathbb{R}$ is a periodic Lipschitz continuous function. Then

$$|a + v'(y)| = \sqrt{(\overline{H}(p) - b f(y))^2 - b^2}.$$

It is not hard to derive that

(1) when $|a| \le \int_0^1 \sqrt{(M - bf(y))^2 - b^2} \, dy$,

$$\overline{H}(p) = M = |b| + \max_{\mathbb{R}} b f;$$

(2) when $|a| > \int_0^1 \sqrt{(M-b\,f(y))^2-b^2}\,dy$, \overline{H} is given by the following implicit formula

$$|a| = \int_0^1 \sqrt{(\overline{H}(p) - b f(y))^2 - b^2} \, dy.$$

The computation is similar to that in [67] for $H(p,x) = |p|^2 + W(x)$. The detail is left to interested readers.

3.3. Growth law of $\overline{H}(p)$ in 2D cellular flows. In general, the behavior of $\overline{H}(p)$ as a function of p is quite complicated and does not possess any formula in closed form. Here we focus on how $\overline{H}(p)$ depends on the large flow intensity, an extensively studied issue in combustion literature. Precisely speaking, for A>0, let $V(x)\to AV(x)$ and consider the corresponding $\overline{H}(p,A)$ in the cell problem

$$|p + Dv| + AV(x) \cdot (p + Dv) = \overline{H}(p, A)$$
 in \mathbb{R}^n .

Question 1. What is the growth pattern of $\overline{H}(p,A)$ as $A \to +\infty$?

To derive a meaningful result, we need to look at physically interesting examples of V. The first is a 2D Hamiltonian flow, the cellular flow with a typical form:

$$V(x_1, x_2) = (-H_{x_2}, H_{x_1}).$$

Here the stream function $H = \sin x_1 \sin x_2$. As mentioned before, this is an integrable form (after suitable rotation) of the ABC flow [7, 35, 47], a steady periodic solution to the 3D Euler equation. Using (2.8) and the control formulation (3.2), it was proved in [117] that for any unit vector $p \in \mathbb{R}^2$

(3.6)
$$\frac{A\pi(|p_1|+|p_2|)}{2\log A + C_2} \le \overline{H}(p,A) \le \frac{A\pi(|p_1|+|p_2|)}{2\log A + C_1}.$$

Here C_1 and C_2 are two constants independent of A and p. Below is an interesting question:

Question 2. Does there exist a constant C such that

$$\left| \overline{H}(p,A) - \frac{A \pi(|p_1| + |p_2|)}{2 \log A + C} \right| \le O(A^{\alpha})$$

for some $\alpha \in [0,1)$?

This question is closely related to identifying the curvature effect discussed in Section 4

In numerical computation [60] and physical modeling [30,54] of G-equation, a viscosity term is often added (explicitly or implicitly), which leads to the viscous G-equation:

$$-d\Delta G + |DG| + AV(x) \cdot DG = 0.$$

Accordingly, a natural question is to identify the effect of viscosity term in lieu of the curvature term. Let $\overline{H}(d, p, A)$ be the unique constant such that the corresponding cell problem

$$-d\Delta v + |p + Dv| + AV(x) \cdot (p + Dv) = \overline{H}(d, p, A)$$
 in \mathbb{R}^n

has a periodic solution v. Due to the presence of the Δv , the existence of $\overline{H}(d, p, A)$ is well known (see [42]). Surprisingly, it turns out that the viscosity term will dramatically slow down the effective burning velocity. Precisely speaking, Theorem 3.5 was proved in [69].

Theorem 3.5. For fixed d > 0 and $V(x_1, x_2) = (-H_{x_2}, H_{x_1})$ with $H = \sin x_1 \sin x_2$

$$\sup_{A \ge 0} \overline{H}(d, p, A) \le C_d |p|$$

for a constant C_d depending only on d.

Below is the outline of the proof. Integrating both sides of the above cell problem gives

$$\overline{H}(d, p, A) = \int_{\mathbb{T}^n} |p + Dv| \, dx.$$

Accordingly, we need to derive a uniform L^1 bound of Dv. This is done in two steps.

Step 1. Consider periodic solution T of the linear equation

$$-d\Delta T + AV(x) \cdot (p + DT) = 0 \quad \text{in } \mathbb{R}^n.$$

It was first established that L^1 norms of Dv and DT are comparable:

$$\frac{1}{C} \|DT\|_{L^1(\mathbb{T}^2)} \le \|Dv\|_{L^1(\mathbb{T}^2)} \le C \|DT\|_{L^1(\mathbb{T}^2)}$$

for a constant C independent of A.

Step 2. Prove that the L^1 norm of Dv is uniformly bounded

$$||DT||_{L^1(\mathbb{T}^2)} \le C.$$

This is achieved by (1) carefully using interior decay estimates of $||DT||_{L^2}$ established in [85]; and (2) delicate estimates of $||DT||_{L^1}$ near the boundary $\{H=0\}$, especially near corners, via suitable change of variables.

3.4. Growth law of $\overline{H}(p)$ in the ABC flow and Kolmogorov flow. In 3D incompressible flows, due to the presence of chaotic structures, it becomes much more challenging to analyze the dependence of $\overline{H}(p,A)$ on A. The following asymptotic result was proved in [118]:

Theorem 3.6.

$$\lim_{A \to +\infty} s_T(p, A)/A = \max_{\sigma \in \Lambda} \int_{\mathbb{T}^n} p \cdot V(x) d\sigma$$
$$= \max_{\dot{\xi} = V(\xi)} \limsup_{T \to +\infty} \xi(T) \cdot p/T.$$

where Λ is the collection of all Borel probability measures on \mathbb{T}^n which are invariant under the flow $\dot{\xi} = V(\xi)$.

Below is a basic question.

Question 3. For a given 3D periodic incompressible flow, determine whether

$$\lim_{A \to +\infty} \frac{s_T(p, A)}{A} > 0$$

or, equivalently, whether $\overline{H}(p,A)$ grows linearly with respect to A.

This seemingly simple problem is, in general, very challenging when $n \geq 3$ since it requires identifying the long-time behavior of trajectories of $\dot{\xi} = V(\xi)$ that usually has chaotic structures. In particular, to prove the linear growth might require finding unbounded trajectories with predictable long time behavior (e.g., periodic or quasi-periodic when projected on the flat torus \mathbb{T}^n). For example, if there is a periodic trajectory with a rotation vector not perpendicular to p, then (3.7) holds.

Now let us turn to a well-known example of 3D incompressible flow introduced by Arnold, Beltrami, and Childress, the so-called ABC flow [7, 35, 47]. For $x = (x_1, x_2, x_3) \in \mathbb{R}^3$,

$$V(x) = (A\sin x_3 + C\cos x_2, B\sin x_1 + A\cos x_3, C\sin x_2 + B\cos x_1),$$

where A, B and C are three positive constants. Note that the parameter A here is not the flow intensity. If one of them is zero, the flow is up to a $\pi/4$ rotation the integrable cellular flow. The ABC flow is a periodic steady solution of the Euler equation. In fact, the ABC flow satisfies the Beltrami property $(\nabla = (\frac{\partial}{\partial x_1}, \frac{\partial}{\partial x_2}, \frac{\partial}{\partial x_3})$ denotes the gradient operator):

$$\nabla \times V := \operatorname{curl}(V) = V.$$

Using the following identity in vector calculus

$$(V\cdot\nabla)V=\nabla\frac{1}{2}|V|^2-V\times(\nabla\times V),$$

we have that the second term on the right hand side vanishes and

$$V_t + (V \cdot \nabla)V = (V \cdot \nabla)V = -\nabla P$$
 and $\nabla \cdot V = 0$,

where the pressure $P = -\frac{1}{2}|V|^2$. Hence ABC flow is a steady state of the 3D incompressible Euler equation in fluid mechanics, see [35,47] for more discussion of its dynamic properties.

In the symmetric case A = B = C = 1, the existence of noncontractable periodic orbits (in the sense stated precisely below) has been proved by using symmetry of the flow [120]:

Theorem 3.7. There exists $t_0 > 0$ and a solution X(t) = (x(t), y(t), z(t)) to the 1-1-1 ABC flow system such that for each $t \in \mathbb{R}$ we have

$$X(t+t_0) = X(t) + (2\pi, 0, 0).$$

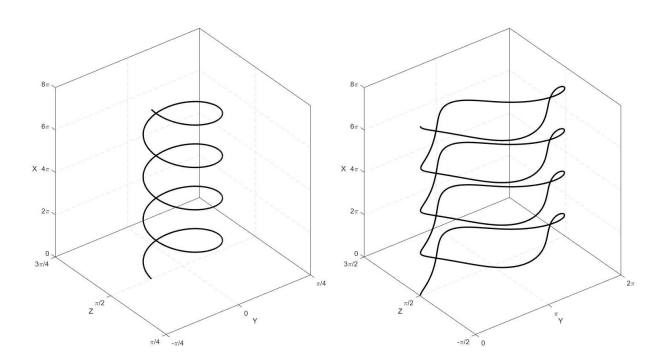


FIGURE 5. Ballistic orbits, periodic (modulo 2π) along x-direction, in 1-1-1 ABC (left) and Kolmogorov (right) flows.

Then Y(t) = (z(t), x(t), y(t)) and Z(t) = (y(t), z(t), x(t)) are clearly also solutions and satisfy

$$Y(t+t_0) = Y(t) + (0, 2\pi, 0)$$
 and $Z(t+t_0) = Z(t) + (0, 0, 2\pi)$.

The Kolmogorov flow with more chaotic phase space [29] is

$$(3.8) V(x, y, z) = (\sin z, \sin x, \sin y),$$

for which similar ballistic orbits exist [58], e.g., those that extend along each coordinate direction. See Figure 5 for an illustration of two such orbits extending in a spiral manner in the x direction. For related studies, we refer to [58,77].

Thanks to control formula (3.2), an immediate corollary is that in the 1-1-1 ABC and Kolmogorov flows, the effective burning velocity grows linearly with respect to the flow intensity A, i.e.,

$$\lim_{A \to +\infty} \frac{\overline{H}(p, A)}{A} > 0 \quad \text{for all unit vector } p \in \mathbb{R}^3.$$

Moreover, for p along a coordinate direction [58],

(3.9)
$$\frac{2\pi}{t_0} A + \frac{2\pi}{t_0 \|V\|_{\infty}} \le \overline{H}(p, A) \le \|V \cdot p\|_{\infty} A + 1.$$

With numerical estimates of period values t_0 from the 1-1-1 ABC and Kolmorogov flows, the following inequalities [58] follow from (3.9):

$$1.942A + 0.793 \le \overline{H} \le 2A + 1$$
, (1-1-1 ABC);
 $0.414A + 0.239 \le \overline{H} \le A + 1$, (Kolmogorov).

Connection with the Weinstein conjecture. To find noncontractible periodic orbits for general Beltrami flows is much more difficult and is closely related to the well known Weinstein conjecture due to the relation between Beltrami and Reeb vector fields (see [78]). Given a Beltrami flow V(x), we can define a one-form on the flat torus \mathbb{T}^3 :

$$a = V(x) \cdot dx$$
.

Since $\operatorname{curl}(V) = \lambda V$ for a constant $\lambda \neq 0$ (Beltrami property),

$$a \wedge da = \lambda |V(x)|^2 dx_1 \wedge dx_2 \wedge dx_3.$$

Accordingly, $\frac{V}{|V|^2}$ is a Reeb vector field if V is nowhere vanishing. Owing to a celebrated result of Taubes [103], V has at least one unbounded periodic orbit with certain rotation vector q, which implies that

$$\lim_{A \to +\infty} \frac{\overline{H}(p, A)}{A} > 0, \quad \text{if } p \cdot q \neq 0.$$

However, this is not enough to obtain linear growth along every unit direction. Note that Taubes's result does not apply to the 1-1-1 ABC flow that has critical points.

4. Curvature G-equation

Recall the curvature G-equation

(4.1)
$$G_t + \left(1 - d\operatorname{div}\left(\frac{DG}{|DG|}\right)\right)_+ |DG| + V(x) \cdot DG = 0.$$

A fundamental question is to understand how the curvature term influences the prediction of the effective burning velocity. The first step is to rigorously establish the existence of effective burning velocity. Precisely speaking, given a unit direction $p \in \mathbb{R}^n$, let G(x,t) be the unique solution to

(4.2)
$$\begin{cases} G_t + \left(1 - d \operatorname{div}\left(\frac{DG}{|DG|}\right)\right)_+ |DG| + V(x) \cdot DG = 0 \\ G(x,0) = p \cdot x. \end{cases}$$

Question 4. Does there exist constant $\overline{H}(p)$ such that

$$-\lim_{t \to +\infty} \frac{G(x,t) - p \cdot x}{t} = \overline{H}(p) \quad \text{uniformly for } x \in \mathbb{R}^n?$$

Due to the presence of curvature term, this question is much harder than the inviscid case (d = 0).

First, let us review some literature related to the homogenization of mean curvature type equations. In other applications such as crystal growth (e.g. freezing or melting of ice in pure liquid [65]), the curvature effect is also considered and the motion law is given by (without the drift term $V \cdot \vec{n}$ and ()₊ correction)

$$v_{\vec{n}} = a(x) - d\kappa$$

for a continuous positive \mathbb{Z}^n -periodic function a(x). The above formula is known as the Gibbs-Thomson relation. The $()_+$ is not needed in crystal growth since both freezing and melting could occur. Equation (4.4) is the associated equation

(4.4)
$$u_t + \left(a(x) - d \operatorname{div}\left(\frac{Du}{|Du|}\right)\right) |Du| = 0 \quad \text{in } \mathbb{R}^n \times (0, \infty).$$

• When a(x) and Da(x) satisfy the following coercivity condition

$$\min_{\mathbb{R}^n} \{ a^2 - (n-1)d|Da| \} > 0,$$

the existence of effective propagation speed (a corresponding form of (4.3) and full homogenization have been proved in all dimensions [68];

• When n=2, homogenization was proved in [18] for all positive a(x) by a geometric approach. See [15] for a survey on relevant methods. Moreover, counterexamples are constructed there when $n \geq 3$. (See [21, 25, 32, 34, 49, 52, 53, 56] and the references therein for other related works and mathematical models.)

The proofs in [18,68] rely heavily on the coercivity of HJE in the gradient variable. A new approach needs to be developed to deal with the curvature G-equation where coercivity is lost when the flow intensity |V| exceeds the local burning velocity $s_L^0 = 1$, which is the typical scenario in turbulent combustion.

4.1. Existence of average flame speeds in cellular flows. Let $V: \mathbb{R}^2 \to \mathbb{R}^2$ be the steady two dimensional cellular flow, e.g., $V(x) = A(DH(x))^{\perp}$ with stream function $H(x_1, x_2) = \sin(x_1)\sin(x_2)$ and flow intensity A > 0. Theorem 4.1 is the main theorem proved in [50].

Theorem 4.1. For any unit vector $p \in \mathbb{R}^2$ and initial data $G(x,0) = p \cdot x$, there exists a positive number $\overline{H}_A(p)$ such that

$$(4.5) |G(x,t) - p \cdot x + \overline{H}_A(p)t| \le C in \mathbb{R}^2 \times [0,\infty),$$

holds for solution G(x,t) of the curvature G-equation (4.1) with a constant C depending only on d and V. In particular, this implies that

$$-\lim_{t\to\infty}\frac{G(x,t)}{t}=\overline{H}(p)\quad locally\ uniformly\ for\ x\in\mathbb{R}^2.$$

The effective Hamiltonian $\overline{H}_A(p)$ corresponds to the effective burning velocity (turbulent flame speed) in the physics literature [89, 93, 112]. The inequality (4.5) says that to leading order, the solution of curvature G-equation (4.1) from the planar initial data $p \cdot x$ develops into a traveling front $p \cdot x - \overline{H}_A(p)t$.

Sketch of proof. Our proof combines PDE methods with a dynamical analysis of the Kohn–Serfaty deterministic game characterization [63, 64] of (4.1) while utilizing the streamline structure of the cellular flow. To the best of our knowledge, this is the first time that a Lagrangian method has been used to prove homogenization of second order PDEs. For the reader's convenience, we will briefly review key ideas, tools, and steps in the proof. Let us look for a solution to (4.1) of the form $p \cdot x - \overline{H}_A(p)t + v(x)$, where v is the corrector which satisfies the following equation (a.k.a. cell problem) upon substitution:

$$(4.6) \qquad \left(1 - d\operatorname{div}\left(\frac{p + Dv}{|p + Dv|}\right)\right)_{+} |p + Dv| + V(y) \cdot (p + Dv) = \overline{H}_{A}(p)$$

subject to 2π -periodic boundary condition in y. The spatial variable of (4.6) is renamed y from the original x, since (4.6) becomes an independent problem that relates the flow velocity to a large scale constant \overline{H}_A in the direction p. One may view (4.6) as a nonlinear eigenvalue problem with v an eigenfunction ($v\pm$ const. still a solution) and $\overline{H}_A(p)$ an eigenvalue for any given unit vector p.

As in [67], we start with a modified (a.k.a. discount) cell problem:

(4.7)
$$\lambda v + \left(1 - d\operatorname{div}\left(\frac{p + Dv}{|p + Dv|}\right)\right)_{\perp} |p + Dv| + V(y) \cdot (p + Dv) = 0,$$

for a parameter $\lambda > 0$, so that the existence and uniqueness of solution $v = v_{\lambda}$ to (4.7) is known by Perron's method [33]. Also, the comparison principle applies to (4.7) where we evaluate maximum of $v_{\lambda}(x)$ to find

(4.8)
$$\max_{x \in \mathbb{R}^2} |\lambda v_{\lambda}(x)| \le 1 + \max_{\mathbb{R}^2} |V|.$$

Our goal is to show that there exists a positive constant $\overline{H}_A(p)$ such that

(4.9)
$$\lim_{\lambda \to 0} \lambda \, v_{\lambda}(x) = -\overline{H}_{A}(p) \quad \text{uniformly on } \mathbb{R}^{2},$$

thereby showing that (4.6) follows in the $\lambda \downarrow 0$ limit with further estimate on v_{λ} .

In Sections 4.2 and 4.3, we explain the main ideas for proving (4.9) while omitting the subscript A for simplicity. Let C be a constant depending only on d and V. A key inequality we shall establish is

(4.10)
$$\max_{x, y \in [-\pi, \pi]^2} |v_{\lambda}(x) - v_{\lambda}(y)| \le C,$$

which implies the constant limit of (4.9). Due to the curvature term and noncoercivity in the discount cell problem (4.7), it is not clear that the equicontinuity of v_{λ} , a standard yet stronger estimate than (4.10), even holds. Our strategy is: (1) establishing one-way reachability from the associated game dynamics; and (2) leveraging a minimum value principle (Eulerian) to compensate for the lack of full reachability. The proof coherently integrates Lagrangian and Eulerian thinking. It turns out that the game trajectory under player I's strategy more or less reverses the propagation route of flame, hence a generalized method of characteristics is at work.

4.2. Two-player game representation and analysis. The deterministic game representation of Kohn and Serfaty [63] applies to (4.1) on \mathbb{R}^2 as follows. Consider the discrete dynamical system $\{x_n\}_{n=1}^N \subset \mathbb{R}^2$ associated with the game starting from $x_0 = x$. For n = 0, 1, 2, ..., N - 1, $|\vec{\eta}_n| \leq 1$ and $b_n \in \{-1, 1\}$,

$$\begin{cases} x_{n+1} = x_n + \tau \sqrt{2d} \, b_n \, \vec{\eta}_n + \tau^2 \, \vec{\eta}_n^{\perp} - \tau^2 \, V(x_n) \\ x_0 = x. \end{cases}$$

Player I controls direction via $\vec{\eta}_n$ and player II controls sign via b_n . Let g = g(x) be a final payoff function. Player I (II) aims to minimize (maximize) $g(x_N)$. If both players proceed optimally, the value function $u(x, N\tau^2) := g(x_N)$, converges to a solution of (4.1) with initial data g(x): $\lim_{N\tau^2 \to t, \tau \to 0} u(x, N\tau^2) = G(x, t)$. See Remark 4.7 for a high-dimensional version of the game.

Remark 4.2. We shall derive inequalities from one-way reachability in the flow -V(x) via game trajectories $\{x_n\}_{n=1}^N$. A typical scenario to get an upper bound of the game value is for player I to devise a strategy so that the game trajectory, starting at a point P, ends at a point Q in a desired region U in N moves despite any strategy of player II. Then

$$u(P, N\tau^2) \le g(Q) \le \max_{q \in U} g(q).$$

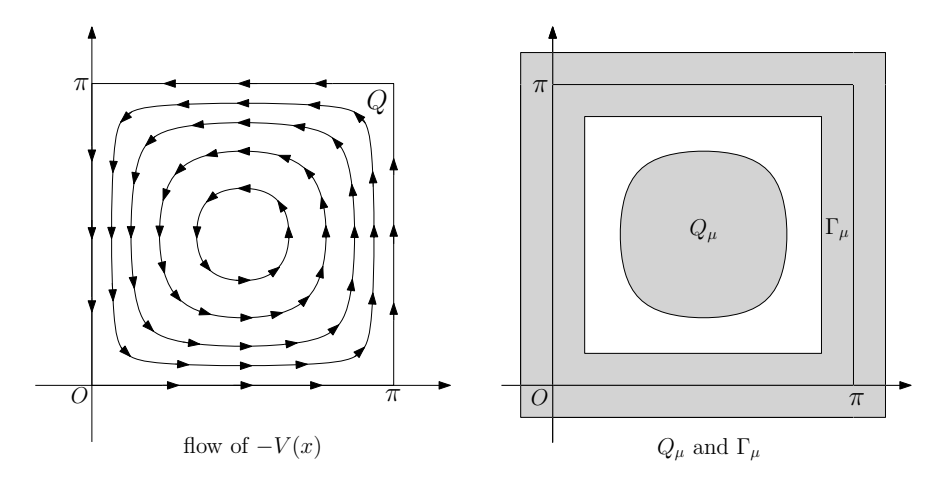


FIGURE 6. Flow lines of -V (left), two domains in the analysis (right): Q_{μ} and Γ_{μ} .

4.2.1. Reachability of game trajectory in and across cells. The one-way reachability property of the game dynamics in the interior of cellular flow, whose quarter-cell with streamline is shown in Figure 6 (left). The quarter-cell $Q = [0, \pi] \times [0, \pi]$ has core $Q_{\mu} = \{x \in Q \mid H(x) > \mu\}$ and boundary region

$$\Gamma_{\mu} = \{x = (x_1, x_2) \in \mathbb{R}^2 \mid \min\{|x_1|, |x_2|, |x_1 - \pi|, |x_2 - \pi|\} < \mu\}.$$

for $\mu \in (0,1]$. Note that Q_{μ} is -V flow invariant.

Lemma 4.3. Let $\mu \in (0,1)$, then the level curve $\{x \in Q \mid H(x) = \mu\}$ is reachable from $P_1 \in Q_\mu$ within time T_1 depending only on V. Each point $P_2 \in \{x \in Q \mid H(x) = \mu\}$ is reachable from P_1 within time $C(1 + |\log \mu|)$ for a constant C depending only on V.

The proof is based on construction of a game trajectory in Figure 7. The reachability is only one way. If P_1 is near the center of Q where $H(P_1)$ is close to 1 and the curvature on the level curve there exceeds 1, it is *not* reachable from P_2 . This is different from the inviscid case (d=0) where any two points are mutually reachable.

The game trajectory can go across the quarter-cell boundary and reach any adjacent quarter-cell. More precisely,

Lemma 4.4. There exists $\mu_0 > 0$ and $T_0 > 0$ depending only on d and V such that the set $Q_{2\mu_0}$ is reachable from each point $x \in \Gamma_{\mu_0}$ within time T_0 .

The crucial part of Lemma 4.4 is that if the game trajectory is in the outside portion of the quarter-cell boundary layer $\Gamma_{\mu_0} \cap Q^c$, it can pass the boundary and go inside Q, as shown in Figure 8, where $S := (0,1)^2$, $W_{\alpha,\delta} := [-\alpha,\alpha] \times [\delta,1-\delta]$, for $\alpha > 0$ and $\delta \in (0,\frac{1}{2})$. The proof relates an inward optimal game trajectory with the outward motion of the zero level set through a PDE comparison argument.

Based on Lemma 4.4, one can further show that all quarter cells of cellular flow are reachable by a game trajectory starting from one of them within a finite travel time, which leads to Lemma 4.5.

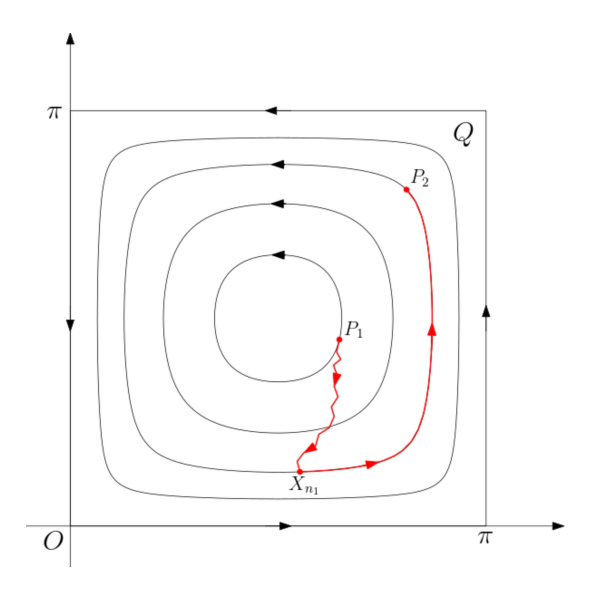


FIGURE 7. a game trajectory (in red) of Lemma 4.3.

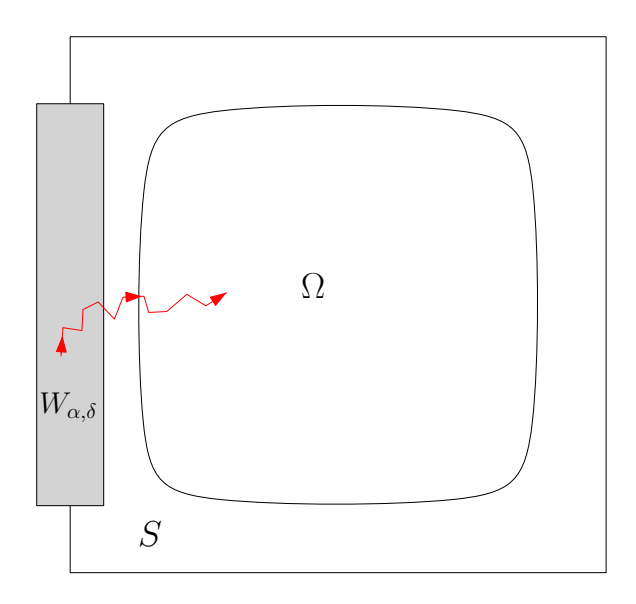


FIGURE 8. Game trajectory reaching a large enough interior region $\Omega \subset S = (0,1)^2$ from a thin rectangular boundary layer $W_{\alpha,\delta} = [-\alpha,\alpha] \times [\delta,1-\delta]$.

Lemma 4.5. Let G(x,t) be the unique solution of (4.1) with $G(x,0) = p \cdot x$. There exist positive constants β and C depending only on d and V such that for all $(x,t) \in \mathbb{R}^2 \times [0,\infty)$,

$$(4.11) G(x,t) - p \cdot x \le -\beta t + C$$

and

(4.12)
$$\max_{x \in \mathbb{R}^2} \lambda \, v_{\lambda}(x) < -\frac{\beta}{2} + \lambda \, C.$$

Inequality (4.11) follows from estimating travel times of game trajectories across cells. Inequality (4.12) comes from constructing a supersolution to a time-dependent variant of the discount cell problem (4.7) via inequality (4.11) where t corresponds to $1/\lambda$ in (4.12). Applying inequality (4.12), we have from equation (4.7) for $\lambda < \beta/(4C)$,

$$(4.13) \qquad \left(1 - d \operatorname{div}\left(\frac{p + Dv_{\lambda}}{|p + Dv_{\lambda}|}\right)\right)_{+} |p + Dv_{\lambda}| + V(y) \cdot (p + Dv_{\lambda}) \ge \beta/4$$

implying the *minimum principle*: the minimum value of $u_{\lambda} := p \cdot x + v_{\lambda}$ in a domain can only be attained on its boundary.

Next we combine minimum principle with one-way reachability of the game trajectory to prove inequality (4.10). First by (4.7)–(4.8), $u = u_{\lambda}$ is a viscosity subsolution of the stationary G-equation:

$$(4.14) \quad \left(1-d \operatorname{div}\left(\frac{Du_{\lambda}}{|Du_{\lambda}|}\right)\right)_{+} |Du_{\lambda}| + V(y) \cdot (Du_{\lambda}) = 1 + \max_{[-\pi,\pi]^{2}} |V|(y) := \alpha,$$

for which the following inequality holds:

$$(4.15) u_{\lambda}(x_0) \le \max_{y \in \bar{S}} u_{\lambda}(y) + \alpha T_0$$

if a bounded set S is reachable from x_0 via a game trajectory within time T_0 , and S is invariant under -V flow. To see (4.15), consider $w := u_{\lambda} - \alpha t$ so that w is a subsolution of G-equation (4.1) with initial data $G(x,0) = u_{\lambda}$. By Remark 4.2 and the comparison principle, $u_{\lambda}(x_0) - \alpha T_0 \leq G(x_0, N \tau^2) \leq \max_{y \in S} u_{\lambda}(y)$. Note that if the game trajectory reaches S before time T_0 , then player I can just choose $\vec{\eta} = 0$, which makes the trajectory flow within S until T_0 due to the flow-invariance of S.

By Lemma 4.3 and equation (4.15), for each point $x \in \partial Q_{\mu}$ and each point $y \in \overline{Q}_{\mu}$, $u_{\lambda}(x) \geq u_{\lambda}(y) - C_{\mu}$ for some constant $C_{\mu} > 0$. Accordingly,

$$\min_{x \in \partial Q_{\mu}} u_{\lambda}(x) \ge \max_{x \in \overline{Q}_{\mu}} u_{\lambda}(x) - C_{\mu}.$$

By minimum principle: $\min_{x \in \partial Q_{\mu}} u_{\lambda}(x) = \min_{x \in \overline{Q}_{\mu}} u_{\lambda}(x)$, and so

(4.16)
$$\max_{x \in \overline{Q}_{\mu}} u_{\lambda}(x) - \min_{x \in \overline{Q}_{\mu}} u_{\lambda}(x) = \max_{x, y \in \overline{Q}_{\mu}} |u_{\lambda}(x) - u_{\lambda}(y)| \le C_{\mu}.$$

With the help of the minimum principle and more delicate analysis, similar estimates hold over the cell boundary and in other quarter cells, and so key inequality (4.10) holds. Theorem 4.1 follows with a sub/supersolution argument [50].

4.3. Existence of H for 2D incompressible flows. The proof for the case of cellular flow in the last subsection can be modified to establish the existence of $\overline{H}(p)$ for a large class of 2D incompressible flows [50], for example, if $V = D^{\perp}H$ for a smooth periodic stream function H that has finitely many non-degenerate critical points whose flow struture is well described in [8]. Also, the constant local burning velocity can be replaced by a positive, continuous and periodic function a(x).

Question 5. Does (4.3) hold for all 2D periodic incompressible flows?

4.4. Bifurcation of effective burning velocity in 3D shear flows. A natural question is whether our robust approach for 2D incompressible flows can be extended to 3D flows. Surprisingly, the effective burning velocity ceases to exist when the flow intensity surpasses a threshold value (bifurcation) for general 3D shear flows, the simplest class of 3D incompressible flows. Meanwhile, the existence of effective burning velocity for 2D shear flows can be easily established by PDE methods. The methods in this section mainly rely on PDE approaches. It is not clear to us how to interpret it by 3D game theory (see Remark 4.7).

Assume that f is a Lipschitz continuous function satisfying

$$(4.17) \{x \in \mathbb{R}^2 : f(x) = \max_{\mathbb{R}^2} f\} = \mathbb{Z}^2, \ \{x \in \mathbb{R}^2 : f(x) = \min_{\mathbb{R}^2} f\} = \mathbb{Z}^2 + \vec{q}$$

for some $\vec{q} \in \mathbb{R}^n$. Here we do not pursue the optimal assumptions on f. Consider the 3D shear flow

$$V(x) = (0, 0, Af(x')),$$

for $x = (x', x_3) \in \mathbb{R}^3$ and $x' \in \mathbb{R}^2$, the constant A > 0 represents the flow intensity. Then equation (4.2) is reduced to

(4.18)
$$\begin{cases} v_t + \left(1 - d\operatorname{div}\frac{p + Dv}{\sqrt{p_3^2 + |p' + Dv|^2}}\right)_+ \sqrt{p_3^2 + |p' + Dv|^2} + Ap_3 f(x') = 0, \\ v(x', 0) = 0 \end{cases}$$

for $G(x,t) = v(x',t) + p \cdot x$ and $p = (p',p_3) \in \mathbb{R}^3$ and $p' \in \mathbb{R}^2$.

For any $p \in \mathbb{R}^3$ with $p_3 \neq 0$, denote by S_H the set of all $A \geq 0$ such that

(4.19)
$$\lim_{t \to \infty} -\frac{G(x,t)}{t} = \overline{H}(p,A) \text{ for all } x \in \mathbb{R}^3$$

for a constant $\overline{H}(p, A)$.

For $\lambda > 0$, let v_{λ} be the periodic continuous viscosity solution to the discount λ -problem on \mathbb{R}^2 :

$$\lambda v_{\lambda} + \left(1 - d \operatorname{div} \frac{p + Dv_{\lambda}}{\sqrt{p_3^2 + |p' + Dv_{\lambda}|^2}}\right) \sqrt{p_3^2 + |p' + Dv_{\lambda}|^2} + Ap_3 f(x') = 0.$$

Then (4.19) is equivalent to

$$\lim_{\lambda \to 0} \lambda \, v_{\lambda}(x') = \overline{H}(p, A), \quad \text{for } x' \in \mathbb{R}^2.$$

Theorem 4.6 is proved in [79]:

Theorem 4.6. For any $p \in \mathbb{R}^3$ with $p_3 \neq 0$,

$$S_H(p) = [0, A_0(p)]$$

for a constant $A_0(p)$ that is continuous with respect to p and $A_0(sp) = A_0(p)$ for any s > 0.

Consequently, $\bar{A} = \min_{p \in \mathbb{R}^3} A_0(p)$ is the bifurcation value for the full homogenization of the corresponding curvature G-equation with uniformly continuous initial data.

Below, we explain how to characterize the bifurcation value $A_0(p)$. Consider the cell problem without ()₊ cutoff:

$$(4.20) \quad \left(1 - d\operatorname{div}\frac{p + D\tilde{v}}{\sqrt{p_3^2 + |p' + D\tilde{v}|^2}}\right) \sqrt{p_3^2 + |p' + D\tilde{v}|^2} + Ap_3 f(x') = \overline{\tilde{H}}(p, A).$$

By the Bernstein technique, it can be shown that, unlike the physical cutoff case, for any given $p \in \mathbb{R}^3$, there exists a constant $\overline{\tilde{H}}(p,A)$ such that the above equation always has a $C^{2,\alpha}$ periodic solution $\tilde{v} = \tilde{v}(x)$. This can be viewed as a special case of [68]. Moreover, $\overline{\tilde{H}}(p,A) - F(p)A$ is strictly decreasing for $A \geq 0$ and $F(p) = \max_{x' \in \mathbb{R}^2} (p_3 f(x'))$.

Apparently, if $\tilde{H}(p,A) \geq AF(p)$, the \tilde{v} is also a solution to the equation with physical cut-off:

$$\left(1 - d\operatorname{div}\frac{p + D\tilde{v}}{\sqrt{p_3^2 + |p' + D\tilde{v}|^2}}\right)_+ \sqrt{p_3^2 + |p' + D\tilde{v}|^2} + Ap_3 f(x') = \overline{\tilde{H}}(p, A).$$

Then $A \in S_H(p)$ and

$$\lim_{t \to \infty} -\frac{G(x,t)}{t} = \overline{\tilde{H}}(p,A).$$

Characterization of $A_0(p)$. For fixed $p \in \mathbb{R}^3$, the bifurcation value $A_0(p)$ is the unique number such that

$$(4.21) \overline{\tilde{H}}(p, A_0(p)) = F(p)A_0(p).$$

Moreover,

$$\overline{H}(p, A) = \overline{\tilde{H}}(p, A)$$
 for $A \in [0, A_0(p)]$.

Hereafter, we reviewed main ideas of the proof. For convenience, we assume that $\max_{\mathbb{R}^2} f = 0$ and $p_3 = 1$. Then F(p) = 0.

Step 1. Using a comparison principle, we can deduce that the set s_H is either $[0, \infty)$ or $[0, A_0(p)]$ for a positive constant $A_0(p)$.

Step 2. We need to show that when A is large enough, $\overline{\tilde{H}}(p,A) < 0$. The main idea is that if that is not true, then we can construct a radial symmetric function v(x) = g(|x|) satisfying

$$\left(1 - d\operatorname{div}\frac{p + Dv}{\sqrt{1 + |p' + Dv|^2}}\right)\sqrt{1 + |p' + Dv|^2} \ge 1 \quad \text{for } r \le |x| \le 2r$$

for small r or equivalently in terms of $g:[r,\frac{1}{2}]\to\mathbb{R}$

$$\sqrt{1+(g')^2}-d\left(\frac{g''}{1+(g')^2}+\frac{g'}{r}\right)\geq 1$$
 for $r\in(r_0,\ 3r_0)$.

Both are in the viscosity sense. Moreover, $g(2r) - g(r) \ge 1$. This will lead to a contradiction when r is small due to the presence of the term $\frac{g'}{r}$ on the left-hand side. We note in passing that for the 2D shear flow, such a term is absent.

Step 3. Finally we need to verify the characterization (4.21), which will provide the continuous dependence on p. It suffices to show that if $\lim_{\lambda\to 0} \lambda v_{\lambda}(x) = 0$, then $\overline{\tilde{H}}(p,A) = 0$. This can be done in two steps. Let $u_{\lambda}(x) = v_{\lambda}(x) + p' \cdot x$.

Step 4. Employing estimates of minimal surface-type equations established in [100], we can show that as $\lambda \to 0$, $u_{\lambda} - u_{\lambda}(0)$ in $\mathbb{R}^2 \backslash \mathbb{Z}^2$ locally and uniformly converges to a function u that is a $C^{2,\alpha}$ solution to

$$\left(1 - d\operatorname{div}\frac{Du}{\sqrt{1 + |Du|^2}}\right)\sqrt{1 + |Du|^2} + Af(x') = 0 \quad \text{in } \mathbb{R}^2 \backslash \mathbb{Z}^2.$$

Step 5. Using integration by parts through suitable test functions, the isolated singularities \mathbb{Z}^2 are proved to be removable at least in the viscosity sense. As a result, compared to the cell problem without cutoff (4.20) leads to $\overline{\tilde{H}}(p,A) = 0$.

Remark 4.7. The Kohn-Serfaty game can be naturally extended to higher dimensions [63]. Consider the 3D case. For $k \geq 1$, at the kth step, let τ be the time step size.

- (1) Player I chooses three vectors u_k , v_k and w_k such that they are mutually perpendicular and $|u_k| = |v_k| = |w_k| \le 1$.
- (2) Player II chooses $b_k = \pm 1$ and $c_k = \pm 1$ to replace (v_k, w_k) by $(b_k v_k, c_k w_k)$.
- (3) Update: $X_k = X_{k-1} + \tau \sqrt{2d} (b_k v_k + c_k w_k) + \tau^2 u_k \tau^2 V(X_{k-1}).$

The above generalization is based on the following fact: given a symmetric matrix S and mutually orthogonal unit vectors u, v and q,

$$u \cdot S \cdot u + v \cdot S \cdot v + q \cdot S \cdot q = tr(S).$$

The other parts are similar to the 2D case. A major difficulty of the 3D game is that it is hard for player I to design a strategy to move between orbits of $\dot{\xi} = -V(\xi)$ due to the lack of topological restrictions. It is not clear to us if the bifurcation phenomenon in shear flows is typical for 3D flows.

Question 6 is the first step towards understanding the role of game theory in 3D flows.

Question 6. Can we find a game theoretic interpretation of the failure of homogenization in 3D shear flows?

Unlike shear flows, turbulent 3D flows often have swirl structures (eddies) which help mix things well. Accordingly, an interesting and challenging problem is Question 7.

Question 7. If V is the ABC flow, do we have

$$S_H(p) = [0, \infty)$$

for all $p \in \mathbb{R}^3$?

- 4.5. Impact of curvature on effective burning velocity. A significant problem in the combustion literature is to understand how the curvature term impacts the prediction of the burning velocity. There is a consensus that curvature slows down flame propagation [93]. Heuristically, this is because the curvature term smooths out the flame front and reduces the total area of chemical reaction. Under the G-equation model, this is equivalent to showing that the effective burning velocity \overline{H} is decreasing with respect to the Markstein number d, which has been observed in combustion experiments [26] and numerical computations [60,62]. We would like to point out that different Markstein number is achieved by the mixture of different fuels in experiments [26]. To establish it rigorously from curvature G-equation is challenging. Below we look at shear flows and 2D cellular flows.
- 4.5.1. Decrease with respect to the Markstein number in shear flows. Theorem 4.8 is the first mathematically rigorous result in this direction obtained in [72] for 2D shear flows.

Theorem 4.8. Let V(x) = (0, f(x')) for $x = (x_1, x') \in \mathbb{R}^2$ and f is a nonconstant periodic continuous function. Then for any fixed vector $p = (p_1, p_2) \in \mathbb{R}^2$ with $p_2 \neq 0$ and $h(d) = \overline{H}(p, d)$,

$$h'(d) \le 0$$
 for $d > 0$

and

$$h'(d) < 0$$
 when d is close to 0.

In particular, this implies that

$$\overline{H}(P,d) < \overline{H}(P,0).$$

Sketch of proof. For 2D shear flows, the effective burning velocity $\overline{H}(p,d)$ always exists and

$$\overline{H}(p,d) = \max \left\{ \overline{\tilde{H}}(p,d), F(p) \right\}.$$

If d is small, $\overline{H}(p,d) = \overline{\tilde{H}}(p,d)$. Here $F(p) = \max_{x' \in \mathbb{R}} (p_2 f(x'))$ and $\overline{\tilde{H}}(p,d)$ is from (4.20) without ()₊ correction. Hence it is enough to show that for fixed unit vector p, $\overline{\tilde{H}}(p,d)$ is strictly decreasing with respect to d

Step 1. For convenience, write

$$E(d) = \overline{\tilde{H}}(p, d).$$

Without loss of generality, we may assume that $p_2 = 1$. Then the cell problem is reduced to an ODE satisfied by $\phi(x') = p_1 + \tilde{v}'(x')$ for $x' \in \mathbb{R}$,

$$-\frac{d\phi'}{1+\phi^2} + \sqrt{1+\phi^2} + f(x') = E(d).$$

Taking derivative on both sides with respect to d, we obtained a linear ODE satisfied by $F = \phi_d$,

$$-dF'(x') + b(x')F = E'(d)(1+\phi^2) + \phi'.$$

Here
$$b(x') = \frac{2d\phi'\phi}{1+\phi^2} + \phi\sqrt{1+\phi^2}$$
.

Step 2. Due to the periodicity of F, E'(d) can be expressed by complicated integrations involving ϕ and ϕ' . Then E'(d) < 0 can be proved by establishing the following delicate inequality

$$e^{T} \int_{0}^{T} f(t) e^{-t} \int_{0}^{t} g(f(s)) e^{s} ds dt + \int_{0}^{T} f(t) e^{-t} \int_{t}^{T} g(f(s)) e^{s} ds dt$$

$$\geq (e^{T} - 1) \int_{0}^{T} f(t) g(f(t)) dt + \frac{\theta}{2} \int_{[0,T]^{2}} |f(t) - f(s)|^{2} dt ds$$

for any continuous positive function $f \in C([0,T])$ and $g \in C^1((0,L])$ for $L = \max_{[0,T]} f$ satisfying $g' \leq -\theta$ for some $\theta \geq 0$.

Step 3. To prove the above inequality, we look at a suitable discrete form where the question is reduced to finding maximum points of functions of finitely many variables. Hence the conclusion can be derived by the simple fact that the gradient vanishes at maximum points.

Note that the proofs in [72] heavily depend on 1D (or $x' \in \mathbb{R}$). Hence a natural question is Question 8.

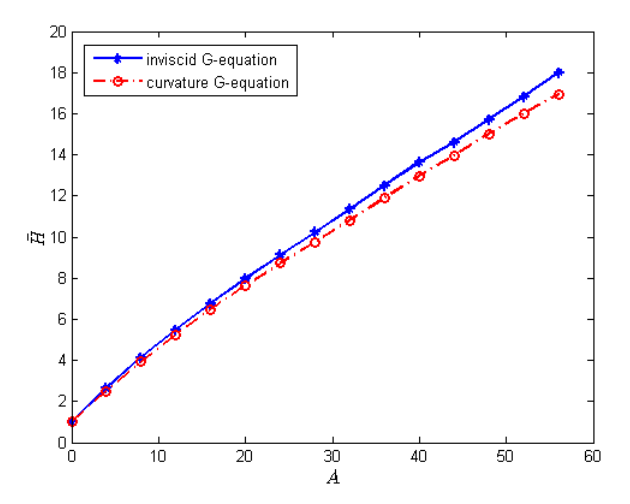


FIGURE 9. Comparison of the homogenized Hamiltonian function in the cellular flow amplitude A without curvature ($\overline{H}(p, 0, A)$, blue line-star) and with curvature ($\overline{H}(p, 0.1, A)$, red dashed-line-circle) by a finite difference method [70].

Question 8. Consider 3D shear flow $V(x_1, x_2, x_3) = (0.0, f(x_1, x_2))$ and the associated $E(d) = \overline{\tilde{H}}(p, d)$ for $p = (p', 1) \in \mathbb{R}^3$. Do we have

for d > 0 and nonconstant f?

4.5.2. Slow down in 2D cellular flows. In case of 2D cellular flow, numerical computation at d=0.1 and different values of A (Figure 9) suggests that for fixed flow intensity

$$(4.22) \hspace{3.1em} \overline{H}(p,d,A) < \overline{H}(p,0,A)$$

and the gap

$$\overline{H}(p,0,A) - \overline{H}(p,d,A)$$

increases as A increases.

It remains a very interesting question to prove (4.22) rigorously. Due to the lack of smooth solutions, we cannot take the derivative of the equation to track the change with respect to d as for the shear flows, i.e., the PDE method in Section 4.4 does not work. Accordingly, the only available tool we have is the game theory interpretation. However, to prove (4.22) might require accurate analysis of the game trajectory, which is particularly difficult given the hidden nonlinear stochastic nature of the game. One hopes that when the flow intensity A gets large (the typical scenario in turbulent combustion), the subtle curvature effect might be amplified and become easier to capture. Thus, a more realistic question is Question 9.

Question 9. Do we have

$$\lim\inf_{A\to\infty}(\overline{H}(p,0,A)-\overline{H}(p,d,A))>0,$$

or do we actually have the limit equal to ∞ ?

We can show that $\overline{H}(p, d, A)$ also grows like $O(A/\log A)$ as in the inviscid case (d=0). Hence, finding the constant (if it exists) in Question 2 seems relevant.

Recall that G-equation with a strain term has the following form:

(5.1)
$$G_t + \left(1 + d \frac{DG \cdot S(x) \cdot DG}{|DG|^2}\right)_+ |DG| + V(x) \cdot DG = 0,$$

where $S = \frac{DV + (DV)^{\top}}{2}$ is the strain rate tensor. This is a noncoercive and nonconvex Hamilton–Jacobi equation (HJE). Again, we consider the existence of effective burning velocity and its dependence on the constant d and flow intensity. It is well known that solutions to nonconvex first-order HJEs can be interpreted by deterministic two-person differential games [55] which will play important roles in our analysis.

5.1. Shear flows. Consider the (n+1)-dimensional shear flow

$$V(x) = (0, 0, \dots, 0, f(x'))$$

for $x = (x', x_{n+1}) \in \mathbb{R}^{n+1}$ and $x' \in \mathbb{R}^n$. Then for $p = (p', 1) \in \mathbb{R}^{n+1}$, the corresponding cell problem is reduced to

$$\left(1 + \frac{d(p'+Dv) \cdot Df}{1 + |p'+Dv|^2}\right)_+ \sqrt{1 + |p'+Dv|^2} + f(x') = \overline{H}(p',d).$$

First, let $\overline{\tilde{H}}(p',d)$ be the effective Hamiltonian when the ()₊ correction is absent:

$$\left(1 + \frac{d(p' + D\tilde{v}) \cdot Df}{1 + |p' + D\tilde{v}|^2}\right) \sqrt{1 + |p' + D\tilde{v}|^2} + f(x') = \overline{\tilde{H}}(p', d).$$

The existence follows directly from [67]. Since Df = 0 when f attains maximum, it is easy to see that for all $d \ge 0$

$$\min_{p' \in \mathbb{R}^n} \overline{\tilde{H}}(p', d) \ge 1 + \max_{\mathbb{R}^n} f.$$

Hence \tilde{v} is also a solution to

$$\left(1 + \frac{d(p'+D\tilde{v})\cdot Df}{1+|p'+D\tilde{v}|^2}\right)_+ \sqrt{1+|p'+D\tilde{v}|^2} + f(x') = \overline{\tilde{H}}(p',d).$$

Accordingly, $\overline{\tilde{H}}(p',d) = \overline{H}(p',d)$, i.e., the cell problems with or without the ()₊ corrections are the same for shear flows. Hence we write

(5.2)
$$\left(1 + \frac{d(p'+Dv) \cdot Df}{1 + |p'+Dv|^2}\right) \sqrt{1 + |p'+Dv|^2} + f(x') = \overline{H}(p',d).$$

Here the corresponding Hamiltonian is

$$H(P,y) = \sqrt{1+|P|^2} + \frac{dP \cdot Df(y)}{\sqrt{1+|P|^2}}$$

for $(P, y) \in \mathbb{R}^n \times \mathbb{R}^n$. Note that H is not convex in the P variable. When n = 1, H is quasiconvex in P, which is not true when $n \geq 2$.

An interesting question is how the presence of the strain rate term impacts the value of effect burning velocity \overline{H} . Numerical results show that \overline{H} is decreasing with respect to the Markstein number d [60]. This is consistent with Theorem 5.1 which says that for 2D shear flows it reduces the value of $\overline{H}(p',d)$.

Theorem 5.1. Assume that n=1 and fix $p' \in \mathbb{R}$. Then $\overline{H}(p',d)$ is strictly decreasing with respect to $d \geq 0$ when $\overline{H}(p',d) > 1 + \max_{\mathbb{R}} f = \min_{p \in \mathbb{R}^n} \overline{H}(p,d)$.

Proof. For simplicity, write $E(d) = \overline{H}(p',d)$ and u(x) = p'x + v(x) for $x \in \mathbb{R}$. Then

(5.3)
$$\left(1 + \frac{du'f'}{1 + |u'|^2}\right) \sqrt{1 + |u'|^2} + f(x') = E(d).$$

Suppose that $E(d) > 1 + \max_{\mathbb{R}} f$. Note that for fixed $x \in \mathbb{R}$, the Hamiltonian is

$$H(p,x) = \sqrt{1+p^2} + \frac{dpf'(x)}{\sqrt{1+p^2}}$$

for $(p,x) \in \mathbb{R} \times \mathbb{R}$. Then the derivative of H with respect to p has the form

$$H_p(p,x) = \frac{p}{\sqrt{1+p^2}} + \frac{df'(x)}{(\sqrt{1+p^2})^3} = \frac{p(1+p^2) + df'(x)}{(\sqrt{1+p^2})^3}.$$

Apparently, for fixed x there exists a unique p = p(x) such that $H_p(p(x), x) = 0$. Then H attains minimum at p = p(x) and $H_p(p, x) < 0$ when p < p(x) and $H_p(p, x) > 0$ when p > p(x). Thus H^{-1} is a well-defined smooth function on either $(-\infty, p(x)]$ or $[p(x), \infty)$. Since

$$\min_{p \in \mathbb{R}} H(p, x) \le H(0, x) = 1 < E(d) - f(x),$$

we have either

$$u'(x) > \max\{0, p(x)\}$$
 for a.e. $x \in \mathbb{R}$

or

$$u'(x) < \min\{0, p(x)\}$$
 for a.e. $x \in \mathbb{R}$.

Therefore u must be smooth due to the strict monotonicity of H on either side of p = p(x). Without loss of generality, we assume that

$$u'(x) > \max\{0, p(x)\}$$
 for all $x \in \mathbb{R}$.

Then for fixed x

$$H_p(u'(x), x) > 0$$
 and $u'(x) = H^{-1}(E(d) - f(x), x)$.

Here for fixed x, $H^{-1}(\cdot, x)$ is the inverse map of $H(\cdot, x)$ for $p \ge p(x)$. Let g(x) = u'(x) > 0. Taking derivative of (5.3) with respect to d says that

$$H_p(g(x), x)g_d + \frac{gf'}{\sqrt{1+g^2}} = E'(d).$$

Since $h(x) = \frac{1}{g(1+g^2)} > 0$ and

$$H_p(g(x), x) = \frac{g}{\sqrt{1+g^2}} (1 + dh(x)f'(x)) > 0,$$

we have that

$$g_d = \frac{E'(d) - \frac{gf'}{\sqrt{1+g^2}}}{H_n}.$$

Thanks to $\int_0^1 g_d(x) dx = 0$,

$$E'(d) \int_0^1 \frac{1}{H_p(g(x), x)} dx = \int_0^1 \frac{\frac{gf'}{\sqrt{1+g^2}}}{H_p} dx.$$

Then

$$\frac{\frac{gf'}{\sqrt{1+g^2}}}{H_p} = \frac{f'(x)}{1 + dh(x)f'(x)},$$

so

$$\int_{0}^{1} \frac{\frac{gf'}{\sqrt{1+g^{2}}}}{H_{p}} dx = \int_{0}^{1} \frac{f'(x)}{1 + dh(x)f'(x)} dx$$

$$= \int_{0}^{1} \frac{f'(x)}{1 + dh(x)f'(x)} dx - \int_{0}^{1} f'(x) dx$$

$$= -\int_{0}^{1} \frac{dh(x)(f'(x))^{2}}{1 + dh(x)f'(x)} dx < 0.$$

Question 10. Does Theorem 5.1 hold for n = 2 (or 3D shear flows)?

5.2. **2D** cellular flows. Let

$$(5.4) V(x) = (-H_{x_2}, H_{x_1})$$

for $x = (x_1, x_2) \in \mathbb{R}^2$ and $H = \sin x_1 \sin x_2$. The corresponding strain tensor is $S = \begin{pmatrix} -\Phi & 0 \\ 0 & \Phi \end{pmatrix}$ for $\Phi(x) = \cos x_1 \cos x_2$. The strain G-equation with linear initial data then takes form of

(5.5)
$$\begin{cases} G_t + \left(1 - Ad\Phi(x) \frac{|G_{x_1}|^2 - |G_{x_2}|^2}{|DG|^2}\right)_+ |DG| + AV(x) \cdot DG = 0 \\ G(x, 0) = p \cdot x. \end{cases}$$

Here $A \geq 0$ represents the flow intensity. We expect the existence of effective burning velocity for cellular flows to be established by a strategy similar to that in Section 4 using two-player differential game (revisited in Section 5.3): (1) first prove some one way reachability; and then (2) use the minimum value principle to take care of the other direction. The argument will be simpler for the strain G-equation due to the deterministic nature of its game dynamics valid in all dimensions. On the other hand, compared with the curvature G-equation, one analytical disadvantage of the strain G-equation is the lack of clear connection between the value of the strain term and the geometric structure of the streamlines.

Question 11. Does the effective burning velocity exist in (5.5) for general incompressible periodic flows in all dimensions?

Expressing the associated Hamiltonian

$$H(p,x) = \left(1 - Ad\Phi(x)\frac{|p_1|^2 - |p_2|^2}{|p|^2}\right)_+ |p| + AV(x) \cdot p$$

in a min-max or max-min form of differential game (see (5.6) or (5.7) in Section (5.3) is not easy. It is helpful to first consider a simplified Hamiltonian such as

$$\tilde{H}(p,x) = (|p| - Ad\Phi(x)(|p_1| - |p_2|))_+ + AV(x) \cdot p$$

when applying a game theory interpretation and then employ comparison principle to control solutions to the strain G-equation.

For mathematical interest, let us also consider the equation without "+" correction

$$\begin{cases} \tilde{G}_t + \left(1 - Ad\Phi(x) \frac{|\tilde{G}_{x_1}|^2 - |\tilde{G}_{x_2}|^2}{|D\tilde{G}|^2}\right) |D\tilde{G}| + AV(x) \cdot D\tilde{G} = 0 \\ \tilde{G}(x,0) = p \cdot x. \end{cases}$$

It was proved in [119] that there are different ranges of A in terms of the existence and non-existence of effective Hamiltonian. This is quite different from the strain G-equation where the existence of effective burning velocity is expected to hold for all A>0. For simplicity, we state the result for $p=e_1=(1,0)$ below.

Theorem 5.2. There exists $0 < A_0 < A_1$ such that

(i) (Homogenization and propagation range). If $A \in [0, A_0)$ for

$$A_0 = \frac{1}{d \max_{x \in \mathbb{R}^n} ||S(x)||},$$

then the effective Hamiltonian

$$\lim_{t \to \infty} -\frac{\tilde{G}(x,t)}{t} = \overline{H}(e_1, A) \quad \text{for all } x \in \mathbb{R}^2$$

exists and is positive. The proof is similar to that of the basic case $(s_l = 1)$ [116].

(ii) (Homogenization and trapping range). There exists $A_1 > 0$ such that when $A \ge A_1$,

$$\lim_{t\to\infty} -\frac{\tilde{G}(x,t)}{t} = 0 \quad \textit{for all } x\in\mathbb{R}^2.$$

The proof is based on a very delicate analysis of the game dynamics (in Section 5.3) and the streamline structure of cellular flow.

(iii) (Intermediate nonhomogenization range). There exists $A \in [A_0, A_1)$ such that the effective Hamiltonian does not exist, i.e.,

$$\lim_{t\to\infty} -\frac{\tilde{G}(x,t)}{t}$$
, if it exists, depends on x.

More precisely, the limit (if it exists) is nonpositive when x is very close to integer points \mathbb{Z}^2 and is positive when x is away from those integers points.

5.3. Two-person differential game for first order nonconvex HJEs. We revisit the two-person zero sum differential game representation for first order nonconvex HJEs [55] based on notations and formulations from [40]. For simplicity, we only consider HJEs for front propagation:

$$\begin{cases} u_t + H(Du, x) = 0, & \text{on } \mathbb{R}^n \times (0, \infty), \\ u(x, 0) = g(x), \end{cases}$$

and refer to [40] for general HJEs. The equations in [40] are formulated as terminal value problems. To be consistent with other parts of the paper, we adopt the initial value problem. Assume that

(5.6)
$$H(-p,x) = \max_{y \in Y} \min_{z \in Z} \{ f(x,y,z) \cdot p \} \text{ for all } (x,p) \in \mathbb{R}^n \times \mathbb{R}^n$$

(5.7) $H(-p,x) = \min_{z \in Z} \max_{u \in Y} \{ f(x,\eta,\mu) \cdot p \} \quad \text{for all } (x,p) \in \mathbb{R}^n \times \mathbb{R}^n.$

or

Here Y and Z are subsets of \mathbb{R}^n . We also set

- (1) M(t) as the set of measurable functions $[0,t] \to Y$;
- (2) N(t) as the set of measurable functions $[0, t] \to Z$;
- (3) $\Gamma(t)$ as the set of strategies of player I, i.e, nonanticipating mappings $\alpha: N(t) \to M(t)$ satisfying that for all s < t and $z, \tilde{z} \in N(t)$:

$$\begin{cases} z(s) = \tilde{z}(s) & \text{for a.e. } 0 \le s \le t \\ \text{impliesthat} \alpha(z)(s) = \alpha(\tilde{z})(s) & \text{for a.e. } 0 \le s \le t; \end{cases}$$

(4) $\Delta(t)$ as the set of strategies of player II, i.e., nonanticipating mappings $\beta: M(t) \to N(t)$ satisfying that for all s < t and $y, \tilde{y} \in M(t)$:

$$\begin{cases} y(s) = \tilde{y}(s) & \text{for a.e. } 0 \le s \le t \\ \text{impliesthat} \beta(y)(s) = \beta(\tilde{y})(s) & \text{for a.e. } 0 \le s \le t. \end{cases}$$

Given t > 0 and $(y(s), \beta) \in M(t) \times \alpha(t)$ or $(z(s), \alpha) \in N(t) \times \beta(t)$, let $x = x(s) : [0, t] \to \mathbb{R}^2$ be a Lipschitz continuous curve satisfying x(0) = x and

(i) if at each time s, player I moves first by choosing y(s) and player II chooses a corresponding strategy β , then

$$\dot{x}(s) = f(x(s), y(s), \beta(y)(s))$$
 for a.e $s \in (0, t)$;

(ii) if at each time s, player II moves first by choosing z(s) at each time s and player I chooses a corresponding strategy α , then

$$\dot{x}(s) = f(x(s), \alpha(z)(s), z(s))$$
 for a.e $t \in (0, t)$.

In both situations, player I wants to minimize the final payoff g(x(t)) and player II aims to maximize g(x(t)). Assume that both players play optimally, [40, Theorem 4.1] says that

$$u(x,t) = \sup_{\beta \in \Delta(t)} \inf_{y \in M(t)} \{g(x(t))\} \quad \text{if (5.6) holds}$$

or

$$u(x,t) = \inf_{\alpha \in \Gamma(t)} \sup_{z \in N(t)} \{g(x(t))\} \quad \text{if (5.7) holds}.$$

In particular, if H satisfies the Issacs condition [55]:

$$\max_{y \in Y} \min_{z \in Z} \{ f(x, y, z) \cdot p \} = \min_{z \in Z} \max_{y \in Y} \{ f(x, \eta, \mu) \cdot p \},$$

then

$$\sup_{\beta \in \Delta(t)} \inf_{y \in M(t)} \{g(x(t))\} = \inf_{\alpha \in \Gamma(t)} \sup_{z \in N(t)} \{g(x(t))\},$$

which says that the game value is the same regardless of which player moves first as long as both of them play optimally.

Compared with the curvature G-equation, the strain G-equation has advantages (first order with a game formula in \mathbb{R}^n) and disadvantages (harder to discern useful strategies for estimates and leverage streamline properties in the flow). A reasonable first step towards the open question in Section 5.2 via the differential game here is to look at flows where some knowledge of streamlines is available, such as cellular flows in 2D, and ABC and Kolmogorov flows in 3D.

6. Other passive scalar combustion models

In this section we briefly review two other ways to model the turbulent flame speeds based on the following reaction-diffusion-advection (RDA) equation

(6.1)
$$T_t + V(x) \cdot DT = d \Delta T + \frac{1}{\tau_r} f(T),$$
$$T(x,0) = T_0(x), \quad x \in \mathbb{R}^n,$$

where T represents the reactant temperature, D is the spatial gradient operator, V(x) is a prescribed fluid velocity, d is the molecular diffusion constant, f is a nonlinear function and τ_r is the reaction time scale. Among different nonlinearities, a popular choice is Fisher–Kolmogorov–Petrovsky–Piskunov (FKPP) reaction. A prototypical example is f(T) = T(1-T) (see [114] for more details). The reaction term f corresponds to the L^1 term $s_l|Du|$ in G-equation model.

- (1) In (6.1), the effective burning velocity along any unit vector $p \in \mathbb{R}^n$ is the minimal spreading speed c_p^* from nonnegative initial data. Similar to G-equation, two active research topics are (1) the existence of c_p^* ; and (2) how it depends on the flow intensity if V is scaled to AV(x). We refer to [10, 11, 17, 31, 46, 51, 71, 80, 82–84, 86, 95–98, 109, 113–115, 126, 127] and references therein, among others. A comparison between (6.1) and G-equation was studied in [118].
- (2) An inviscid model was derived in [73] from (6.1) with FKPP reaction in the scaling regime

$$\kappa = d \, \epsilon, \ \tau_r = \epsilon \quad \text{and} \quad V = V \left(\frac{x}{\epsilon^{\alpha}} \right)$$

for $\alpha \in (0,1)$ and a small $\epsilon > 0$ by assuming that the flame thickness is much smaller than the turbulence scale. Then the turbulent flame speed along direction p is given by

$$c_T(p) = \inf_{\lambda > 0} \frac{f'(0) + \overline{H}(p\lambda)}{\lambda}.$$

Here $\overline{H}(p)$ is the effective Hamiltonian associated with the following cell problem: for each $p \in \mathbb{R}^n$, there is a unique number $\overline{H}(p)$ such that the inviscid quadratic HJE equation below has a periodic viscosity solution $w(x) \in C^{0,1}(\mathbb{T}^n)$

(6.2)
$$d|p + Dw|^2 + V(x) \cdot (p + Dw) = \overline{H}(p) \quad \text{in } \mathbb{R}^n.$$

We refer to [37] and [117] for comparison with the G-equation model.

If the flame is burning through a material at rest (i.e., V=0) and $f(r) = \frac{1}{\epsilon}g(\frac{r}{\epsilon})$ for a suitable nonnegative function $g \in C_0^1(0,1)$, reaction-diffusion equation (6.1) tends to an interesting free boundary problem as $\epsilon \to 0$ ([20])

(6.3)
$$\begin{cases} u_t - \Delta u = 0 & \text{in } \{u > 0\} \\ |Du| = 1 & \text{in } \partial \{u > 0\}. \end{cases}$$

Existence and regularity of the solution u have been studied in [20], among others. Moreover, this singular limit and the corresponding homogenization problem has been considered in [16, 17] for a generalized version when (6.3) has an advection

term in the homogeneous media. (Also, see [19] for a survey on other scaling related to the stationary version of the above equation and phase transition problems.)

7. Basic Stochastic G-Equation

The existence of average front speeds in the basic G-equation

(7.1)
$$G_t + |DG| + V(x, \omega) \cdot DG = 0,$$

with a stochastic incompressible vector field $V(x,\omega)$ (where ω is the random sampling variable) has been studied via homogenization [14,23,81]. Theoretical and numerical studies in physics and engineering literature include [28,59,60,101,121,124], among others.

Due to lack of compactness, stochastic flows or random media have extreme behavior and cause additional difficulty on the large scale so that homogenization can fail even in the coercive and convex Hamilton-Jacobi equations ([115, Chapter 4] and references therein). Hence technical assumptions on the random field are needed. Stochastic homogenization of HJE in several space dimensions was first proved in [102] and [92] in the coercive, convex, and stationary ergodic setting. The strategy is to first find suitable subadditive quantities, then apply the subadditive ergodic theorem instead of relying on corrector problems to obtain an effective quantity (often equal to the dual of the effective Hamiltonian), and finally recover the effective Hamiltonian via duality. In statistical mechanics, such a method was developed in the study of first passage percolation through the connectivity function to establish the existence of limiting shapes [2,61], which can be viewed as a discrete propagation problem associated with the Hamiltonian $H(p,x) = a(x,\omega)|p|$. This method, however, does not work for a nonconvex HJE that requires completely different approaches and might fail in general [45, 125]. To the best of our knowledge, the only available method to homogenize nonconvex HJEs under the general stationary ergodic setting is to first identify the shape of the effective Hamiltonian and then build customized correctors [5,6,48,91]. When i.i.d type assumptions are imposed, approaches from first passage percolation can be used [4,45]. We would like to mention that the periodic setting is a special case of the general stationary ergodic situation, but periodicity is on the opposite side of decorrelation.

7.1. Homogenization analysis. As in the case of periodic flows, the control formulation and the reachability concept play an essential role. The key quantity is the minimal travel time $\tau(x,y,\omega)$ for the control trajectory $\xi_{\alpha}(s)$ to connect two points $x=\xi_{\alpha}(0)$ and $y=\xi_{\alpha}(\tau)$. In two dimensions, the incompressible flow is given by $V=(-\Psi_y,\Psi_x)$, Ψ a stream function. Under stationarity, ergodicity, and a third order moment condition of Ψ (i.e., $\mathbb{E}[|\Psi(0)|^3]<+\infty$), the scaled $\tau(0,r\,y,\omega)$ as a function of $r\in\mathbb{R}$ is subadditive, and $r^{-1}\,\tau(0,r\,y,\omega)$ converges at large r to a deterministic function $\overline{q}=\overline{q}(y)$ almost surely by the subadditive ergodic theorem in [81]. Then homogenization similar to Theorem 3.3 holds with probability one based on control formula (3.2). The effective Hamiltonian is recovered from \overline{q} by duality (Legendre transform):

(7.2)
$$\bar{H}(p) = \sup\{p \cdot y : y \in \mathbb{R}^d, \bar{q}(y) = 1\}.$$

That \bar{H} being convex and homogeneous of degree one follows from (7.2), as it is the supremum of a family of linear functions of p.

In dimensions higher than two, results in [81] extend under certain assumptions of $\tau(x,y,\omega)$ when |x-y| diverges. Through a refined analysis of τ and its long-time behavior along a selected random sequence of times, [23] removed these assumptions and proved homogenization under $V=V(x,\omega)$ being stationary, ergodic, divergence free, and zero mean. The subadditive techniques extend to problems involving time-dependent flows. For space-time flows $V=V(t,x,\omega)$, with a quantitative estimate of reachability of any two points by a controlled path, [14] proved the almost sure homogenization of (7.1) under uniform bound ($\sup_{t,x,\omega}V<\infty$), stationarity, finite time decorrelation, small mean, Lipschitz continuity and incompressibility. As in periodic flows of Section 3, the reachability under control in the stochastic flows is both ways for any two points. The relatively strict finite time decorrelation assumption in [14] has been relaxed to allow the infinite temporal range of dependence of the space-time flow V in a recent work [123] based on a nonautonomous subadditive theorem.

The travel time approach in [23,81] is fully Lagrangian and bypasses the corrector problem entirely. It relies on duality to come back to \bar{H} . The duality is lost however in a nonconvex HJE (e.g., when the strain rate is considered in G-equation), and it is open what would replace duality for a fully Lagrangian (corrector free) method to work.

Question 12. Can homogenization be established for strain G-equation for some interesting stochastic flows? A basic example is 3D random shear flow.

7.2. Formal analysis and numerical and physical experiments. Formal renormalization group and scaling analysis [28, 121] for basic stochastic G-equation (7.1) showed that $\bar{H} = \bar{H}(A)$ scales as $O(A/\sqrt{\log A})$ at large A for a random incompressible flow of the form $AV(x,t,\omega)$ in three dimensions. In aqueous autocatalytic chemical reaction experiments on four different multiscale flows, namely Hele–Shaw, capillary wave, Taylor–Couette, and vibrating-grid flows [1,94,99], the theory [121] and a sublinear power law fit reach good agreement with measurements in the range of flow intensities scaled by s_l (denoted by u'/s_l , u' := A is the flow intensity) in Figure 10.

In view of the asymptotic law $O(A/\log A)$ in BC (cellular) flows [118] and the law O(A) in ABC and Kolmogorov flows [58,120], we see that the presence of continuously many scales in stochastic flow [28,121] indicates the absence of structures such as closed streamlines (in BC/cellular flows) and ballistic orbits (in ABC and Kolmogorov flows) as a plausible explanation of the $O(A/\sqrt{\log A})$ enhancement. A rigorous study awaits to be carried out to discover the mathematics of this long-standing random phenomenon.

Curvature dependence of flame speeds remain an active research topic in combustion science today [62]. With the increasing concern of global warming, new combustion systems aim specifically to reduce or eliminate greenhouse gas emissions. Since carbon dioxide is a key greenhouse factor, fuels without carbon content, such as hydrogen and ammonia, are promising alternatives but come with new challenges, such as widened range of flammability, high flame speed and low activation energy for ignition [107]. In [62], premixed flames subject to turbulent disturbances and harmonic oscillation are studied experimentally and computationally. These flames come from mixtures of methane/hydrogen/air and are stabilized on an oscillating holder to consistently produce harmonic wrinkles for studying curvature effects. The direct numerical simulations are also conducted for a range of flow

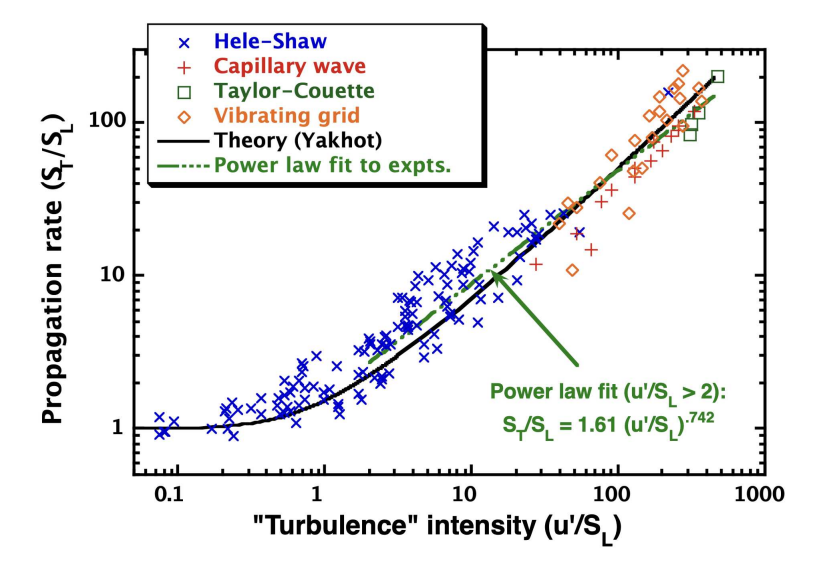


FIGURE 10. Comparison of propagation speeds (s_T/s_l) of wrinkled aqueous autocatalytic reaction fronts in Hele–Shaw, capillary wave, Taylor–Couette and vibrating-grid flows [1, 94, 99] along with a prediction by [121] and a sublinear power-law fit (applied only to data at $u'/s_l > 2$) in the range [0.1, 1000] of scaled flow intensity.

intensities. The turbulent flame speed and the Markstein length are characterized via the basic G-equation as a reduced order model. A power law relating turbulent flame speed to the ensemble-averaged flame curvature in the curved flame regions is observed in [62].

Likewise, flow-induced flame stretch, a fundamental quantity measuring the rate of change of flame surface area, continues to receive attention from experimental measurements to direct simulations (see [108] and references therein).

8. Conclusions

We have reviewed mathematical tools for averaging (homogenizing) level-set G-equations arising in turbulent combustion. As curvature and flame stretch effects are included, the G-equations become nonconvex and noncoercive. We showed how to leverage Lagrangian ideas (e.g., reachability of control and game trajectories) to compensate for the lack of compactness in the Eulerian (viscosity solution) framework to prove the existence and analyze qualitative properties of average flame speeds in prototypical (shear, BC, ABC, and Kolmogorov) flows. We discussed growth laws of flame speeds as flow intensities become large based on the streamline structures of the ambient fluid flows. We explored physical background and proposed open problems for further research in this emerging area of game theoretic analysis of nonconvex and noncoercive geometric PDEs in complex advection.

ACKNOWLEDGMENT

The authors would like to thank Professor Y. Liu at the National Cheng-Kung University at Tainan, Taiwan, for his assistance with numerical computations.

References

- [1] M. Abid, Instabilities of propagating quasi-2D gaseous flames and chemical fronts in narrow channels, PhD thesis, University of Southern California, 1999.
- [2] K. Alexander, J. Chayes, and L. Chayes, The Wulff construction and asymptotics of the finite cluster distribution for two-dimensional Bernoulli percolation, Comm. Math. Phys. 131 (1990), no. 1, 1–50. MR1062747
- [3] P. Andrews, The Rothermel surface fire spread model and associated developments: A comprehensive explanation, Gen. Tech. Rep. RMRS-GTR-371. Fort Collins, CO: U.S. Department of Agriculture, Forest Service, Rocky Mountain Research Station, pages 1–121, 2018.
- [4] S. Armstrong and P. Cardaliaguet, Stochastic homogenization of quasilinear Hamilton– Jacobi equations and geometric motions, J. Eur. Math. Soc. (JEMS) 20 (2018), no. 4, 797–864, DOI 10.4171/JEMS/777. MR3779686
- [5] S. Armstrong, H. Tran, and Y. Yu, Stochastic homogenization of a nonconvex Hamilton– Jacobi equation, Calc. Var. Partial Differential Equations 54 (2015), no. 2, 1507–1524, DOI 10.1007/s00526-015-0833-2. MR3396421
- [6] S. Armstrong, H. Tran, and Y. Yu, Stochastic homogenization of nonconvex Hamilton– Jacobi equations in one space dimension, J. Differential Equations 261 (2016), no. 5, 2702– 2737, DOI 10.1016/j.jde.2016.05.010. MR3507985
- [7] V. Arnol'd, Sur la topologie des écoulements stationnaires des fluides parfaits (French), C.
 R. Acad. Sci. Paris 261 (1965), 17–20. MR180949
- [8] V. Arnol'd, Topological and ergodic properties of closed 1-forms with incommensurable periods (Russian), Funktsional. Anal. i Prilozhen. 25 (1991), no. 2, 1–12, 96, DOI 10.1007/BF01079587; English transl., Funct. Anal. Appl. 25 (1991), no. 2, 81–90. MR1142204
- [9] W. Ashurst and I. Shepherd, Flame front curvature distribution in a turbulent premixed flame zone, Combust. Sci. Tech., 124:115-144, 1997.
- [10] H. Berestycki and F. Hamel, Front propagation in periodic excitable media, Comm. Pure Appl. Math. 55 (2002), no. 8, 949–1032, DOI 10.1002/cpa.3022. MR1900178
- [11] H. Berestycki and F. Hamel, Generalized transition waves and their properties, Comm. Pure Appl. Math. 65 (2012), no. 5, 592–648, DOI 10.1002/cpa.21389. MR2898886
- [12] D. Bradley, How fast can we burn, Proceedings of the Combustion Institute, 24:247–262, 1992.
- [13] D. Burago, Periodic metrics, Representation theory and dynamical systems, Adv. Soviet Math., vol. 9, Amer. Math. Soc., Providence, RI, 1992, pp. 205–210. MR1166203
- [14] D. Burago, S. Ivanov, and A. Novikov, Feeble fish in time-dependent waters and homogenization of the G-equation, Comm. Pure Appl. Math. 73 (2020), no. 7, 1453–1489, DOI 10.1002/cpa.21878. MR4156607
- [15] L. Caffarelli, The homogenization of surfaces and boundaries, Bull. Braz. Math. Soc. (N.S.) 44 (2013), no. 4, 755–775, DOI 10.1007/s00574-013-0033-7. MR3167131
- [16] L. Caffarelli, K.-A. Lee, and A. Mellet, Singular limit and homogenization for flame propagation in periodic excitable media, Arch. Ration. Mech. Anal. 172 (2004), no. 2, 153–190, DOI 10.1007/s00205-003-0299-9. MR2058162
- [17] L. Caffarelli, K.-A. Lee, and A. Mellet, Homogenization and flame propagation in periodic excitable media: the asymptotic speed of propagation, Comm. Pure Appl. Math. 59 (2006), no. 4, 501–525, DOI 10.1002/cpa.20094. MR2199784
- [18] L. Caffarelli and R. Monneau, Counter-example in three dimension and homogenization of geometric motions in two dimension, Arch. Ration. Mech. Anal. 212 (2014), no. 2, 503–574, DOI 10.1007/s00205-013-0712-y. MR3176351
- [19] L. Caffarelli and Y. Sire, Minimal surfaces and free boundaries: recent developments, Bull. Amer. Math. Soc. (N.S.) 57 (2020), no. 1, 91–106, DOI 10.1090/bull/1673. MR4037409
- [20] L. Caffarelli and J. Vázquez, A free-boundary problem for the heat equation arising in flame propagation, Trans. Amer. Math. Soc. 347 (1995), no. 2, 411–441, DOI 10.2307/2154895. MR1260199
- [21] P. Cardaliaguet, P.-L. Lions, and P. Souganidis, A discussion about the homogenization of moving interfaces (English, with English and French summaries), J. Math. Pures Appl. (9) 91 (2009), no. 4, 339–363, DOI 10.1016/j.matpur.2009.01.014. MR2518002

- [22] P. Cardaliaguet, J. Nolen, and P. Souganidis, Homogenization and enhancement for the G-equation, Arch. Ration. Mech. Anal. 199 (2011), no. 2, 527–561, DOI 10.1007/s00205-010-0332-8. MR2763033
- [23] P. Cardaliaguet and P. Souganidis, Homogenization and enhancement of the G-equation in random environments, Comm. Pure Appl. Math. 66 (2013), no. 10, 1582–1628, DOI 10.1002/cpa.21449. MR3084699
- [24] M. Cencini, A. Torcini, D. Vergni, and A. Vulpiani, Thin front propagation in steady and unsteady cellular flows, Phys. Fluids 15 (2003), no. 3, 679–688, DOI 10.1063/1.1541668. MR1958079
- [25] A. Cesaroni and M. Novaga, Long-time behavior of the mean curvature flow with periodic forcing, Comm. Partial Differential Equations 38 (2013), no. 5, 780–801, DOI 10.1080/03605302.2013.771508. MR3046293
- [26] S. Chaudhuri, F. Wu, and C. Law, Scaling of turbulent flame speed for expanding flames with Markstein diffusion considerations, Phys. Rev. E, 88(3):033005, 2013.
- [27] Y. G. Chen, Y. Giga, and S. Goto, Uniqueness and existence of viscosity solutions of generalized mean curvature flow equations, J. Differential Geom. 33 (1991), no. 3, 749–786. MR1100211
- [28] M. Chertkov and V. Yakhot, Huygens front propagation in turbulent fluids, Phys. Rev. Lett, 80:2837–2841, 1998.
- [29] S. Childress and A. Gilbert, Stretch, Twist, Fold: The Fast Dynamo, Lecture Notes in Physics Monographs, No. 37, Springer, 1995.
- [30] P. Clavin, Dynamic behavior of premixed flame fronts in laminar and turbulent flows, Prog. Energy Combust. Sci., 11(1):1–59, 1985.
- [31] P. Constantin, A. Kiselev, A. Oberman, and L. Ryzhik, Bulk burning rate in passive-reactive diffusion, Arch. Ration. Mech. Anal. 154 (2000), no. 1, 53–91, DOI 10.1007/s002050000090. MR1778121
- [32] B. Craciun and K. Bhattacharya, Effective motion of a curvature-sensitive interface through a heterogeneous medium, Interfaces Free Bound. 6 (2004), no. 2, 151–173, DOI 10.4171/IFB/95. MR2079601
- [33] M. Crandall, H. Ishii, and P.-L. Lions, User's guide to viscosity solutions of second order partial differential equations, Bull. Amer. Math. Soc. (N.S.) 27 (1992), no. 1, 1–67, DOI 10.1090/S0273-0979-1992-00266-5. MR1118699
- [34] N. Dirr, G. Karali, and N. Yip, Pulsating wave for mean curvature flow in in-homogeneous medium, European J. Appl. Math. 19 (2008), no. 6, 661–699, DOI 10.1017/S095679250800764X. MR2463225
- [35] T. Dombre, U. Frisch, J. Greene, M. Hénon, A. Mehr, and A. Soward, Chaotic streamlines in the ABC flows, J. Fluid Mech. 167 (1986), 353–391, DOI 10.1017/S0022112086002859. MR851673
- [36] J. Driscoll, Turbulent premixed combustion: Flamelet structure and its effect on turbulent burning velocities, Progress in Energy and Combustion Science, 34:91–134, 2008.
- [37] P. Embid, A. Majda, and P. Souganidis, Comparison of turbulent flame speeds from complete averaging and the G-equation, Phys. Fluids 7 (1995), no. 8, 2052–2060, DOI 10.1063/1.868452. MR1346082
- [38] B. Engquist and P. Souganidis, Asymptotic and numerical homogenization, Acta Numer. 17 (2008), 147–190, DOI 10.1017/S0962492906360011. MR2436011
- [39] L. Evans, Partial differential equations, 2nd ed., Graduate Studies in Mathematics, vol. 19, American Mathematical Society, Providence, RI, 2010, DOI 10.1090/gsm/019. MR2597943
- [40] L. Evans and P. Souganidis, Differential games and representation formulas for solutions of Hamilton-Jacobi-Isaacs equations, Indiana Univ. Math. J. 33 (1984), no. 5, 773-797, DOI 10.1512/iumj.1984.33.33040. MR756158
- [41] L. Evans, The perturbed test function method for viscosity solutions of nonlinear PDE, Proc. Roy. Soc. Edinburgh Sect. A 111 (1989), no. 3-4, 359–375, DOI 10.1017/S0308210500018631. MR1007533
- [42] L. Evans, Periodic homogenisation of certain fully nonlinear partial differential equations, Proc. Roy. Soc. Edinburgh Sect. A 120 (1992), no. 3-4, 245–265, DOI 10.1017/S0308210500032121. MR1159184
- [43] L. Evans, Towards a quantum analog of weak KAM theory, Comm. Math. Phys. 244 (2004), no. 2, 311–334, DOI 10.1007/s00220-003-0975-5. MR2031033

- [44] L. Evans and J. Spruck, Motion of level sets by mean curvature. I, J. Differential Geom. 33 (1991), no. 3, 635–681. MR1100206
- [45] W. Feldman and P. Souganidis, Homogenization and non-homogenization of certain non-convex Hamilton-Jacobi equations, J. Math. Pures Appl. (9) 108 (2017), no. 5, 751–782, DOI 10.1016/j.matpur.2017.05.016. MR3711473
- [46] M. Freidlin, Functional integration and partial differential equations, Annals of Mathematics Studies, vol. 109, Princeton University Press, Princeton, NJ, 1985, DOI 10.1515/9781400881598. MR833742
- [47] S. Friedlander, A. Gilbert, and M. Vishik, Hydrodynamic instability for certain ABC flows, Geophys. Astrophys. Fluid Dynam. 73 (1993), no. 1-4, 97–107, DOI 10.1080/03091929308203622. Magnetohydrodynamic stability and dynamos (Chicago, IL, 1992). MR1289022
- [48] H. Gao, Random homogenization of coercive Hamilton-Jacobi equations in 1d, Calc. Var. Partial Differential Equations 55 (2016), no. 2, Art. 30, 39, DOI 10.1007/s00526-016-0968-9. MR3466903
- [49] H. Gao and I. Kim, Head and tail speeds of mean curvature flow with forcing, Arch. Ration. Mech. Anal. 235 (2020), no. 1, 287–354, DOI 10.1007/s00205-019-01423-3. MR4062478
- [50] H. Gao, Z. Long, J. Xin, and Y. Yu, Existence of an Effective Burning Velocity in a Cellular Flow for the Curvature G-Equation Proved Using a Game Analysis, J. Geom. Anal. 34 (2024), no. 3, 81, DOI 10.1007/s12220-023-01523-3. MR4691893
- [51] J. Gärtner and M. Freidlin, The propagation of concentration waves in periodic and random media (Russian), Dokl. Akad. Nauk SSSR 249 (1979), no. 3, 521–525. MR553200
- [52] Y. Giga, H. Mitake, T. Ohtsuka, and H. Tran, Existence of asymptotic speed of solutions to birth-and-spread type nonlinear partial differential equations, Indiana Univ. Math. J. 70 (2021), no. 1, 121–156, DOI 10.1512/iumj.2021.70.8305. MR4226650
- [53] Y. Giga, H. Mitake, and H. Tran, On asymptotic speed of solutions to level-set mean curvature flow equations with driving and source terms, SIAM J. Math. Anal. 48 (2016), no. 5, 3515–3546, DOI 10.1137/15M1052755. MR3562367
- [54] H. Im, T. Lund, and J. Ferziger, Large eddy simulation of turbulent front propagation with dynamic subgrid models, Phys. Fluids 9 (1997), no. 12, 3826–3833, DOI 10.1063/1.869517. MR1481939
- [55] R. Issacs, Differential games, Wiley, NY, pages 239–249, 1965.
- [56] J. Jang, On optimal rate of convergence in periodic homogenization of forced mean curvature flow of graphs in the laminar setting, arXiv:2303.17113, 2023.
- [57] W. Jing, H. Tran, and Y. Yu, Effective fronts of polygon shapes in two dimensions, SIAM J. Math. Anal. 55 (2023), no. 6, 6764–6777, DOI 10.1137/22M1540971. MR4662766
- [58] C. Kao, Y.-Y. Liu, and J. Xin, A semi-Lagrangian computation of front speeds of G-equation in ABC and Kolmogorov flows with estimation via ballistic orbits, Multiscale Model. Simul. 20 (2022), no. 1, 107–117, DOI 10.1137/20M1387699. MR4372641
- [59] A. Kerstein and W. Ashurst, Propagation rate of growing interfaces in stirred fluids, Phys. Rev. Lett, 68:934–938, 1992.
- [60] A. Kerstein, W. Ashurst, and F. Williams, Field equation for interface propagation in an unsteady homogeneous flow, Physical Review, 37(7):2728–2731, 1988.
- [61] H. Kesten, Percolation theory for mathematicians, Progress in Probability and Statistics, vol. 2, Birkhäuser, Boston, MA, 1982. MR692943
- [62] K. Kim, Y. Kim, A. Aspden, and D. Shin, Ensemble-averaged kinematics of harmonically oscillating turbulent premixed flames, Combustion and Flame, 253(1128125):1–18, 2023.
- [63] R. Kohn and S. Serfaty, A deterministic-control-based approach to motion by curvature, Comm. Pure Appl. Math. 59 (2006), no. 3, 344–407, DOI 10.1002/cpa.20101. MR2200259
- [64] R. Kohn and S. Serfaty, Second-order PDE's and deterministic games, ICIAM 07—6th International Congress on Industrial and Applied Mathematics, Eur. Math. Soc., Zürich, 2009, pp. 239–249, DOI 10.4171/056-1/12. MR2588596
- [65] J. Langer, Instabilities and pattern formation in crystal growth, Reviews of Modern Physics, 52(1):1–28, 1980.
- [66] Z. Lim, J. Li, and A. Morgans, The effect of hydrogen enrichment on the forced response of CH4/H2/air laminar flames, Int. J. Hydrog. Energy, 46:23943–23953, 2021.
- [67] P.-L. Lions, G. Papanicolaou, and S. Varadhan, Homogenization of Hamilton-Jacobi equation, unpublished preprint, circa 1980.

- [68] P.-L. Lions and P. Souganidis, Homogenization of degenerate second-order PDE in periodic and almost periodic environments and applications, Ann. Inst. H. Poincaré C Anal. Non Linéaire 22 (2005), no. 5, 667–677, DOI 10.1016/j.anihpc.2004.10.009. MR2171996
- [69] Y.-Y. Liu, J. Xin, and Y. Yu, Asymptotics for turbulent flame speeds of the viscous G-equation enhanced by cellular and shear flows, Arch. Ration. Mech. Anal. 202 (2011), no. 2, 461–492, DOI 10.1007/s00205-011-0418-y. MR2847532
- [70] Y.-Y. Liu, Turbulent Flame Speeds of G-equations, ProQuest LLC, Ann Arbor, MI, 2012. Thesis (Ph.D.)—University of California, Irvine. MR3034684
- [71] J. Lyu, Z. Wang, J. Xin, and Z. Zhang, A convergent interacting particle method and computation of KPP front speeds in chaotic flows, SIAM J. Numer. Anal. 60 (2022), no. 3, 1136–1167, DOI 10.1137/21M1410786. MR4429419
- [72] J. Lyu, J. Xin, and Y. Yu, Curvature effect in shear flow: slowdown of turbulent flame speeds with Markstein number, Comm. Math. Phys. 359 (2018), no. 2, 515–533, DOI 10.1007/s00220-017-3060-1. MR3783556
- [73] A. Majda and P. Souganidis, Large-scale front dynamics for turbulent reaction-diffusion equations with separated velocity scales, Nonlinearity 7 (1994), no. 1, 1–30. MR1260130
- [74] G. Markstein, Experimental and theoretical studies of flame front stability, J. Aero. Sci, 18:199-209, 1951.
- [75] G. Markstein, Nonsteady flame propagation (ed), AGARDograph, Vol. 75, Elsevier, 1964.
- [76] M. Matalon, On flame stretch, Combust. Sci. Tech., 31:169–181, 1983.
- [77] T. McMillen, J. Xin, Y. Yu, and A. Zlatoš, Ballistic orbits and front speed enhancement for ABC flows, SIAM J. Appl. Dyn. Syst. 15 (2016), no. 3, 1753–1782, DOI 10.1137/16M1059059. MR3549020
- [78] E. Miranda and C. Oms, The singular Weinstein conjecture, Adv. Math. 389 (2021), Paper No. 107925, 41, DOI 10.1016/j.aim.2021.107925. MR4290138
- [79] H. Mitake, C. Mooney, H. Tran, J. Xin, and Y. Yu, Bifurcation of homogenization and nonhomogenization of the curvature G-equation with shear flows, arXiv:2303.16304, 2023.
- [80] G. Nadin and L. Rossi, Transition waves for Fisher-KPP equations with general timeheterogeneous and space-periodic coefficients, Anal. PDE 8 (2015), no. 6, 1351–1377, DOI 10.2140/apde.2015.8.1351. MR3397000
- [81] J. Nolen and A. Novikov, Homogenization of the G-equation with incompressible random drift in two dimensions, Commun. Math. Sci. 9 (2011), no. 2, 561–582. MR2815685
- [82] J. Nolen, J.-M. Roquejoffre, L. Ryzhik, and A. Zlatoš, Existence and non-existence of Fisher-KPP transition fronts, Arch. Ration. Mech. Anal. 203 (2012), no. 1, 217–246, DOI 10.1007/s00205-011-0449-4. MR2864411
- [83] J. Nolen, M. Rudd, and J. Xin, Existence of KPP fronts in spatially-temporally periodic advection and variational principle for propagation speeds, Dyn. Partial Differ. Equ. 2 (2005), no. 1, 1–24, DOI 10.4310/DPDE.2005.v2.n1.a1. MR2142338
- [84] J. Nolen and J. Xin, Asymptotic spreading of KPP reactive fronts in incompressible space-time random flows (English, with English and French summaries), Ann. Inst. H. Poincaré C Anal. Non Linéaire 26 (2009), no. 3, 815–839, DOI 10.1016/j.anihpc.2008.02.005. MR2526403
- [85] A. Novikov, G. Papanicolaou, and L. Ryzhik, Boundary layers for cellular flows at high Péclet numbers, Comm. Pure Appl. Math. 58 (2005), no. 7, 867–922, DOI 10.1002/cpa.20058. MR2142878
- [86] A. Novikov and L. Ryzhik, Boundary layers and KPP fronts in a cellular flow, Arch. Ration. Mech. Anal. 184 (2007), no. 1, 23–48, DOI 10.1007/s00205-006-0038-0. MR2289862
- [87] S. Osher and R. Fedkiw, Level set methods and dynamic implicit surfaces, Applied Mathematical Sciences, vol. 153, Springer-Verlag, New York, 2003, DOI 10.1007/b98879. MR1939127
- [88] S. Osher and J. Sethian, Fronts propagating with curvature-dependent speed: algorithms based on Hamilton-Jacobi formulations, J. Comput. Phys. 79 (1988), no. 1, 12–49, DOI 10.1016/0021-9991(88)90002-2. MR965860
- [89] N. Peters, Turbulent combustion, Cambridge Monographs on Mechanics, Cambridge University Press, Cambridge, 2000, DOI 10.1017/CBO9780511612701. MR1792350
- [90] J. Qian, Two approximations for effective Hamiltonians arising from homogenization of Hamilton-Jacobi equations, UCLA CAM report 03-39, 2003.

- [91] J. Qian, H. Tran, and Y. Yu, Min-max formulas and other properties of certain classes of nonconvex effective Hamiltonians, Math. Ann. 372 (2018), no. 1-2, 91–123, DOI 10.1007/s00208-017-1601-8. MR3856807
- [92] F. Rezakhanlou and J. Tarver, Homogenization for stochastic Hamilton-Jacobi equations, Arch. Ration. Mech. Anal. 151 (2000), no. 4, 277–309, DOI 10.1007/s002050050198. MR1756906
- [93] P. Ronney. Some Open Issues in Premixed Turbulent Combustion, Modeling in Combustion Science (J. Buckmaster and T. Takeno, eds.). In Lecture Notes In Physics, Springer-Verlag, Berlin, volume 449, pages 3–22, 1995.
- [94] P. Ronney, B. Haslam, and N. Rhys, Front propagation rates in randomly stirred media, Physical Review Letters, 74:3804–3807, 1995.
- [95] L. Shen, J. Xin, and A. Zhou, Finite element computation of KPP front speeds in 3D cellular and ABC flows, Math. Model. Nat. Phenom. 8 (2013), no. 3, 182–197, DOI 10.1051/mmnp/20138311. MR3103017
- [96] L. Shen, J. Xin, and A. Zhou, Finite element computation of KPP front speeds in cellular and cat's eye flows, J. Sci. Comput. 55 (2013), no. 2, 455–470, DOI 10.1007/s10915-012-9641-4. MR3044182
- [97] W. Shen, Traveling waves in diffusive random media, J. Dynam. Differential Equations 16 (2004), no. 4, 1011–1060, DOI 10.1007/s10884-004-7832-x. MR2110054
- [98] W. Shen, Variational principle for spreading speeds and generalized propagating speeds in time almost periodic and space periodic KPP models, Trans. Amer. Math. Soc. 362 (2010), no. 10, 5125–5168, DOI 10.1090/S0002-9947-10-04950-0. MR2657675
- [99] S. Shy, R. Jang, and C. Tang, Simulation of turbulent burning velocities using aqueous autocatalytic reactions in a near-homogeneous turbulence, Combust. Flame, 105:54–62, 1996.
- [100] L. Simon, Equations of mean curvature type in 2 independent variables, Pacific J. Math. 69 (1977), no. 1, 245–268. MR454854
- [101] G. Sivashinsky, Renormalization concept of turbulent flame speed, Numerical combustion (Antibes, 1989), Lecture Notes in Phys., vol. 351, Springer, Berlin, 1989, pp. 131–148, DOI 10.1007/3-540-51968-8-80. MR1037592
- [102] P. Souganidis, Stochastic homogenization of Hamilton-Jacobi equations and some applications, Asymptot. Anal. 20 (1999), no. 1, 1–11. MR1697831
- [103] C. Taubes, The Seiberg-Witten equations and the Weinstein conjecture, Geom. Topol. 11 (2007), 2117–2202, DOI 10.2140/gt.2007.11.2117. MR2350473
- [104] H. Tran, Hamilton-Jacobi equations—theory and applications, Graduate Studies in Mathematics, vol. 213, American Mathematical Society, Providence, RI, [2021] ©2021, DOI 10.1090/gsm/213. MR4328923
- [105] S. Tu, Rate of convergence for periodic homogenization of convex Hamilton-Jacobi equations in one dimension, Asymptot. Anal. 121 (2021), no. 2, 171–194, DOI 10.3233/asy-201599. MR4198478
- [106] H. Tran and Y. Yu, Differentiability of effective fronts in the continuous setting in two dimensions, International Mathematics Research Notices, 2023, https://doi.org/10.1093/ imrn/rnad212.
- [107] S. Verhelst and T. Wallner, Hydrogen-fueled internal combustion engines, Progress in Energy & Combustion Sci, 35(6):490–527, 2009.
- [108] H. Wang, E. Hawkes, J. Ren, G. Chen, K. Luo, and J. Fan, 2-D and 3-D measurements of flame stretch and turbulence-flame interactions in turbulent premixed flames using DNS, J. Fluid Mech. 913 (2021), Paper No. A11, 27, DOI 10.1017/jfm.2020.1171. MR4223830
- [109] Z. Wang, J. Xin, and Z. Zhang, DeepParticle: learning invariant measure by a deep neural network minimizing Wasserstein distance on data generated from an interacting particle method, J. Comput. Phys. 464 (2022), Paper No. 111309, 15, DOI 10.1016/j.jcp.2022.111309. MR4428792
- [110] J. Wehr and J. Xin, Front speed in the Burgers equation with a random flux, J. Statist. Phys. 88 (1997), no. 3-4, 843–871, DOI 10.1023/B:JOSS.0000015175.70862.77. MR1467633
- [111] F. Williams, Combustion theory, 2nd edition. Benjamin Cummings, Menlo Park, CA, 1985.
- [112] F. Williams, Turbulent Combustion. In: The Mathematics of Combustion. Society for Industrial and Applied Math, 1985.
- [113] J. Xin, Existence of planar flame fronts in convective-diffusive periodic media, Arch. Rational Mech. Anal. 121 (1992), no. 3, 205–233, DOI 10.1007/BF00410613. MR1188981

- [114] J. Xin, Front propagation in heterogeneous media, SIAM Rev. 42 (2000), no. 2, 161–230, DOI 10.1137/S0036144599364296. MR1778352
- [115] J. Xin, An introduction to fronts in random media, Surveys and Tutorials in the Applied Mathematical Sciences, vol. 5, Springer, New York, 2009, DOI 10.1007/978-0-387-87683-2. MR2527020
- [116] J. Xin and Y. Yu, Periodic homogenization of the inviscid G-equation for incompressible flows, Commun. Math. Sci. 8 (2010), no. 4, 1067–1078. MR2744920
- [117] J. Xin and Y. Yu, Sharp asymptotic growth laws of turbulent flame speeds in cellular flows by inviscid Hamilton–Jacobi models, Ann. Inst. H. Poincaré C Anal. Non Linéaire 30 (2013), no. 6, 1049–1068, DOI 10.1016/j.anihpc.2012.11.004. MR3132416
- [118] J. Xin and Y. Yu, Asymptotic growth rates and strong bending of turbulent flame speeds of G-equation in steady two-dimensional incompressible periodic flows, SIAM J. Math. Anal. 46 (2014), no. 4, 2444–2467, DOI 10.1137/130929990. MR3228465
- [119] J. Xin and Y. Yu, Front quenching in the G-equation model induced by straining of cellular flow, Arch. Ration. Mech. Anal. 214 (2014), no. 1, 1–34, DOI 10.1007/s00205-014-0751-z. MR3237880
- [120] J. Xin, Y. Yu, and A. Zlatoš, Periodic orbits of the ABC flow with A=B=C=1, SIAM J. Math. Anal. **48** (2016), no. 6, 4087–4093, DOI 10.1137/16M1076241. MR3580814
- [121] V. Yakhot, Propagation velocity of premixed turbulent flames, Combust. Sci. Tech, 60:191–241, 1988.
- [122] Y. Yu, High degeneracy of effective Hamiltonian in two dimensions, Ann. Inst. H. Poincaré C Anal. Non Linéaire 39 (2022), no. 1, 201–223, DOI 10.4171/aihpc/6. MR4412068
- [123] Y. Zhang and A. Zlatoš, Homogenization for space-time-dependent KPP reaction-diffusion equations and G-equations, Calc. Var. Partial Differential Equations 62 (2023), no. 9, Paper No. 248, 22, DOI 10.1007/s00526-023-02589-1. MR4655793
- [124] J. Zhu and P. Ronney, Simulation of front propagation at large non-dimensional flow disturbance intensities, Combustion Science and Technology, 100(1):183–201, 1994.
- [125] B. Ziliotto, Stochastic homogenization of nonconvex Hamilton-Jacobi equations: a counterexample, Comm. Pure Appl. Math. 70 (2017), no. 9, 1798–1809, DOI 10.1002/cpa.21674. MR3684310
- [126] A. Zlatoš, Sharp asymptotics for KPP pulsating front speed-up and diffusion enhancement by flows, Arch. Ration. Mech. Anal. 195 (2010), no. 2, 441–453, DOI 10.1007/s00205-009-0282-1. MR2592283
- [127] A. Zlatoš, Generalized traveling waves in disordered media: existence, uniqueness, and stability, Arch. Ration. Mech. Anal. 208 (2013), no. 2, 447–480, DOI 10.1007/s00205-012-0600x. MR3035984

DEPARTMENT OF MATHEMATICS, UNIVERSITY OF CALIFORNIA, IRVINE, CALIFORNIA 92697 Email address: jack.xin@uci.edu

Department of Mathematics, University of California, Irvine, California 92697 $\it Email\ address:\ yifengy@uci.edu$

Department of Aerospace and Mechanical Engineering, University of Southern California, Los Angeles, California 90089

Email address: ronney@usc.edu